STUDIES ON LASERS AND LASER DEVICES

CO-PRINCIPAL INVESTIGATORS:

S. E. Harris
A. E. Siegman
J. F. Young

Final Report

for

NASA Grant NSG-7619

National Aeronautics and Space Administration

Washington, D.C.

for the period

1 April 1979 – 31 March 1980

G.L. Report No. 3132

May 1980

Edward L. Ginzton Laboratory
W. W. Hansen Laboratories of Physics
Stanford University
Stanford, California 94305

(NASA-CR-163144) STUDIES OF LASER AND LASER DEVICES Final Report, 1 Apr. 1979 - 31 Mar. 1980 (Stanford Univ.) 34 p HC A03/MF A01 CSCL 20E

N80-24604

Unclas
G3/36 21511

I. INTRODUCTION

The goal of this grant was to pursue research on the generation of tunable visible, infrared, and ultraviolet light, and on the control of this light by means of novel mode-locking and modulation techniques. The grant, and the program, was a continuation of NASA Grant NGL-05-020-103. Active projects during the year included an analysis of mode-locked and frequency-doubled lasers, a study of energy storage and extraction using metastable atomic levels, the first observation of laser action using an atomic pair absorption process, and the development of a tunable VUV source for spectroscopic studies.

II. SUMMARY OF RESEARCH

A. Energy Storage and Extraction Using Metastable Levels

(R. W. Falcone, G. A. Zdasiuk, J. F. Young, and S. E. Harris)

The objective of this project was to demonstrate the use of atomic metastable states as energy storage media for potential use as high energy lasers and Raman pulse compressors. In particular, we have demonstrated that the barium $6s5d\,^3D$ levels can be optically pumped (via an indirect path) and that these levels have long storage times. We have found that it is possible to transfer ~ 90% of the ground state atoms into the $6s5d\,^3D$ manifold, and to maintain this population for storage times on the order of tens of microseconds at densities of 10^{16} atoms/cm^3. These conditions correspond to a stored energy density of approximately 2 Joules/litre. We have measured the storage time as a function of the barium ground state density and as a function of inert buffer gas densities. We have also observed laser action from a barium excited state to the ground state on the 7911 Å ^3P-^1S intercombination line and also on the ^1P-^1S resonance line at $\lambda = 5535$ Å. These results point strongly to the possibility that the individual $6s5d\,^3D$ sublevels may be inverted relative to the ground state. If this is the case, the Ba system is potentially a very practical Raman medium for upconverting HF lasers from the 2.7-2.9 μm region to the near IR at 7500-8000 Å.

B. Atomic Pair Absorption and Inversion

(R. W. Falcone, G. A. Zdasiuk, J. F. Young, and S. E. Harris)

During the grant period we have demonstrated the use of a novel optical pumping technique based on "atomic pair absorption" as a practical means of populating atomic energy levels. The term "atomic pair absorption" refers to a process whereby two colliding atoms simultaneously absorb a single photon at a frequency corresponding to the sum energy of two levels in the separated atoms. Atomic pair absorption has been observed in barium-thallium mixtures using white light sources.[1] By the use of more intense laser pumping sources we have found that it is possible to construct atomic pair absorption pumped lasers. The details of this work are given in the attached paper "Pair Absorption-Pumped Barium Laser" (see Appendix A).

---

[1] J. C. White, G. A. Zdasiuk, J. F. Young, and S. E. Harris, Optics Lett. 4, 137 (1979).

C. Development of a Tunable, Narrowband VUV Light Source

(J. E. Rothenberg, J. F. Young, and S. E. Harris)

The spontaneous anti-Stokes VUV light source was proposed by Harris[1] in 1977 and first demonstrated by Zych, et al.[2] in 1978, and is a convenient technique for generating intense, pulsed, narrowband, incoherent VUV radiation. The practicality of this source was demonstrated by Falcone, et al.[3] who used it as a tunable spectroscopic source to measure the isotopic shift, and absolute energies, of the ^{3}He and ^{4}He 1s2s $^1S_0$ states with a resolution of 60 μeV. This represented the first direct measurement of the isotopic shift and illustrated the potential of this technique for performing high-resolution VUV spectroscopy without the limitations of traditional VUV apparatus: the lack of bright sources, and the low efficiency and resolution of VUV spectrometers.

Falcone, et al. in essence performed an emission spectroscopy experiment using the anti-Stokes source. The goal of this project is to develop this source and to apply it to absorption spectroscopy of high lying atomic levels. The practical requirement is to produce a tunable source of high intensity which has an overwhelming majority of its energy in a narrow bandwidth, thus eliminating the need for a (lossy) VUV spectrometer.

A schematic of the source and its energy level diagram are shown in Fig. 1. The tunable, visible pump laser illuminates a length L of a He

---

[1] S. E. Harris, Appl. Phys. Lett. 31, 498 (1977).

[2] L. J. Zych, et al., Phys. Rev. Lett. 40, 1493 (1978).

[3] R. W. Falcone, et al., Optics Lett. 3, 162 (1978).

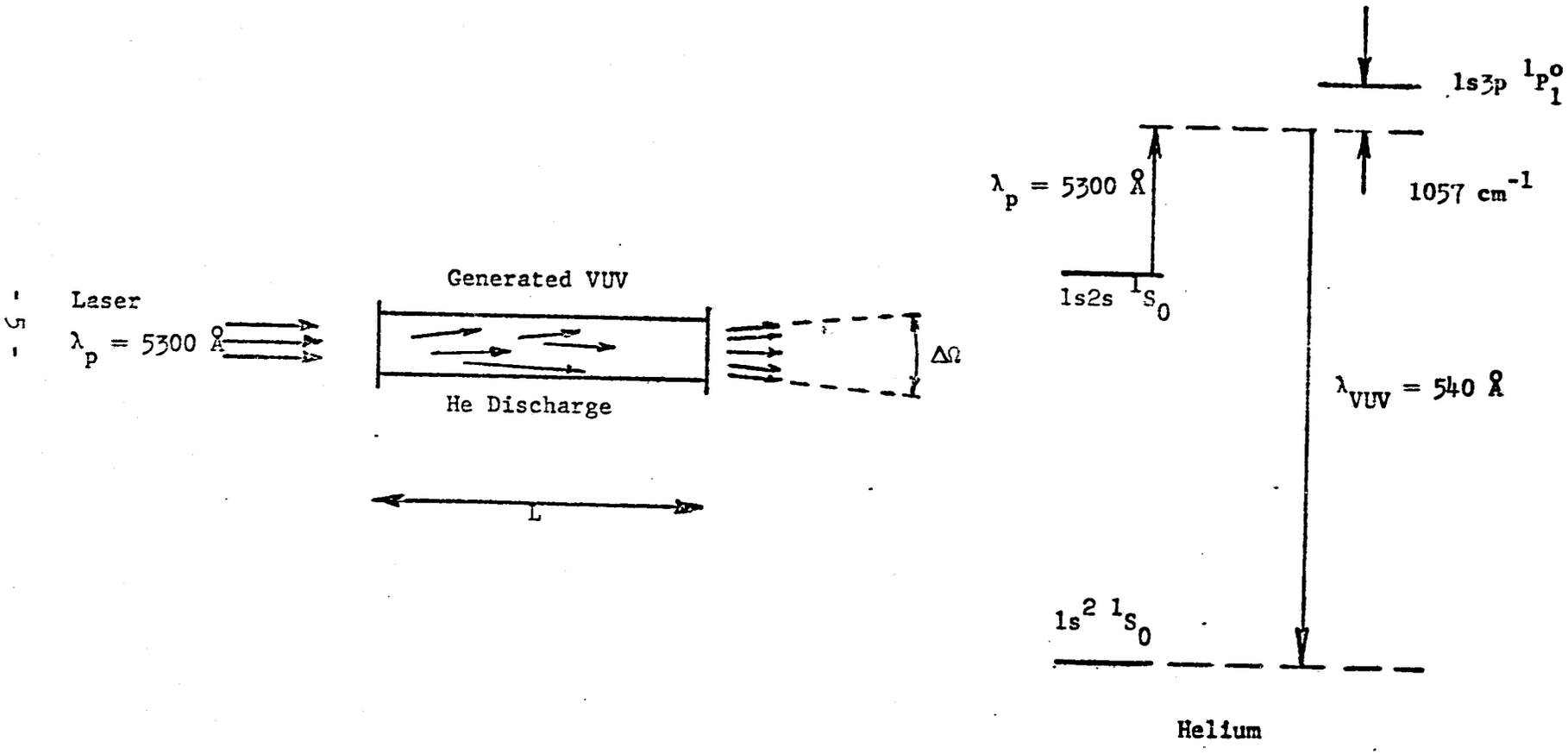

Fig. 1: He anti-Stokes VUV source.

discharge. The anti-Stokes generation process is merely a scattering process; a fraction of the incident photon flux is scattered at the tunable sum frequency $\omega_{1s2s} + \omega_p$ into 4π steradians. The number of generated VUV photons is

$$n_{VUV} = n_{pump} \frac{d\sigma}{d\Omega} N_{1s2s} L$$

where n_{pump} is the number of incident pump photons, N_{1s2s} is the He 1s2s metastable density, $d\sigma/d\Omega$ is the differential cross section for anti-Stokes scattering, and L is the interaction length. The fraction of the generated photons which are actually used in a particular experiment will depend on the effective solid angle $\Delta\Omega$.

The differential scattering cross section depends strongly on the frequency of the applied pump wave, becoming very large when the VUV frequency approaches a resonance line. Initially, we proposed to pump with radiation in the range of 5300 Å and to scatter off the 1s2s $^1S_0$ He level excited by a dc discharge. The critical parameter of the source is the ratio of the anti-Stokes light to the background He resonance line radiation at 584 Å. Therefore, we have been investigating the optimization of the ratio of the anti-Stokes light to the background radiation using different discharge geometries to maximize N_{1s2s} , L , and the collection angle $\Delta\Omega$. We have found that a hollow cathode discharge and a positive column discharge are comparable in these respects.

We have measured this ratio using a flashlamp pumped dye laser which provides peak powers of a few kW as our pump source (see Fig. 2). The anti-Stokes light is seen superimposed on the background radiation over the range

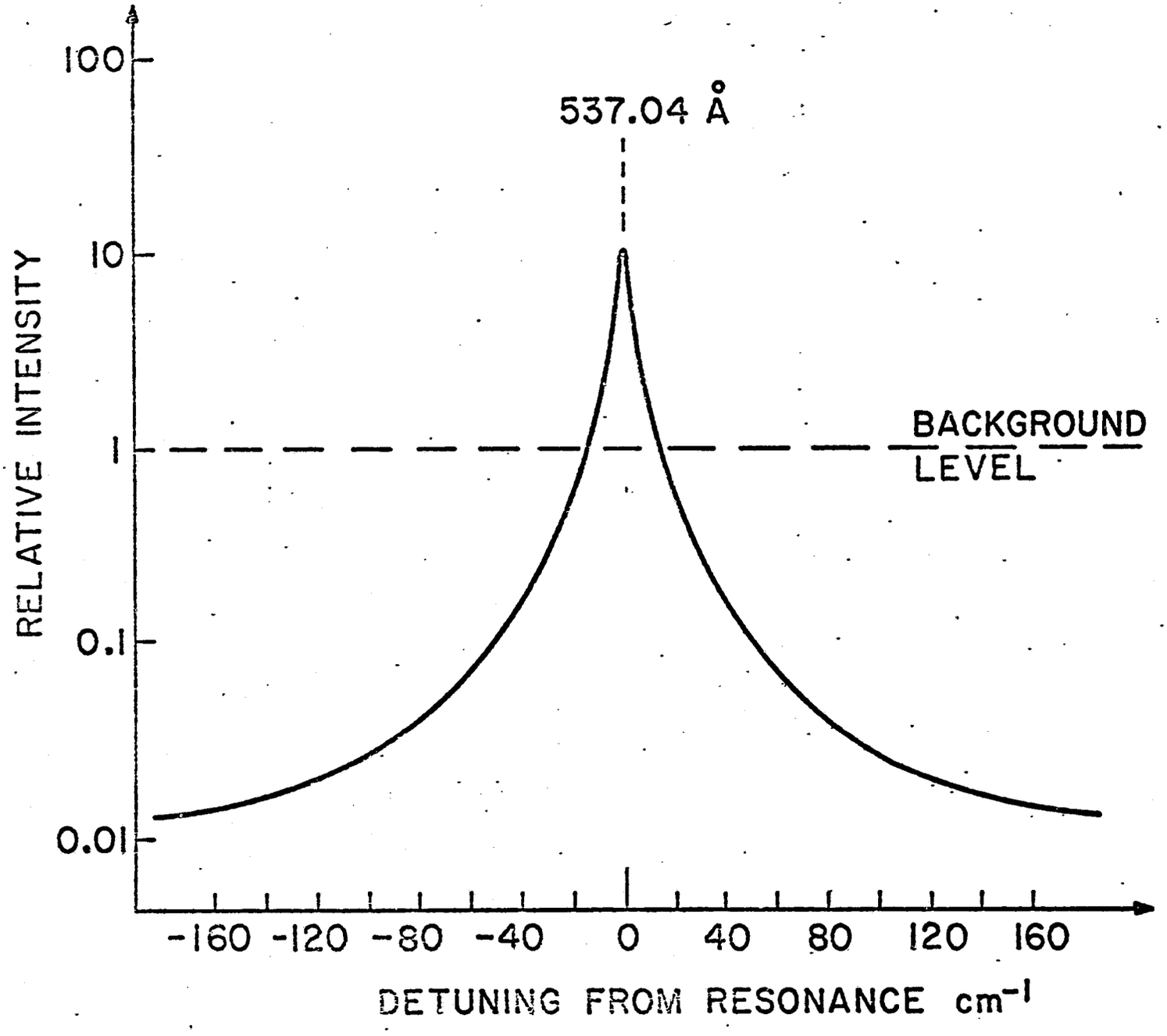

Fig. 2--Anti-stokes brightness vs. pump laser detuning from resonance.

shown in the figure. Outside of this range the fluctuations of the background exceed the anti-Stokes intensity making its observation impossible. However, we will be using a Nd:YAG system capable of producing MW peak powers which would allow observation of the generated anti-Stokes light over the entire range of available dye lasers ($\sim$ 50,000 cm^{-1}). In order to use this laser we have developed a detector with a high work function cathode which will not detect scattered visible laser radiation (at high laser powers this radiation can be comparable to the anti-Stokes light).

As a preliminary test of the Nd:YAG system we have used its second harmonic (5320 Å) at a peak power of 5 MW as our pump laser. This corresponds to a detuning of 1100 cm^{-1} (3 Å) from the resonance at 537.04 Å. The result was an observed anti-Stokes signal five times brighter than the background radiation. We believe this is confirmation that the source will be useful over the broad tuning range of available dyes.

The bandwidth of the generated anti-Stokes light is equal to the convolution of the pump laser bandwidth and the Doppler width of the metastable storage state. In our case this is only a few cm^{-1}, making the resolution and spectral brightness of the device much better than conventional laboratory sources. In the future we propose using this technique to measure the linewidth of the innershell excitation of K $3p^5 4s5s$. An energy level diagram is shown in Fig. 3 and an experimental schematic is shown in Fig. 4. There are good theoretical grounds for believing that the linewidth is relatively narrow, and thus, that the lifetime may be long enough so that it can be used in a VUV laser. To date, this linewidth has not been resolved. Generally, the linewidths of innershell excitations are very large because they are prone to Auger or "autoionizing" decay. This very fast decay occurs when

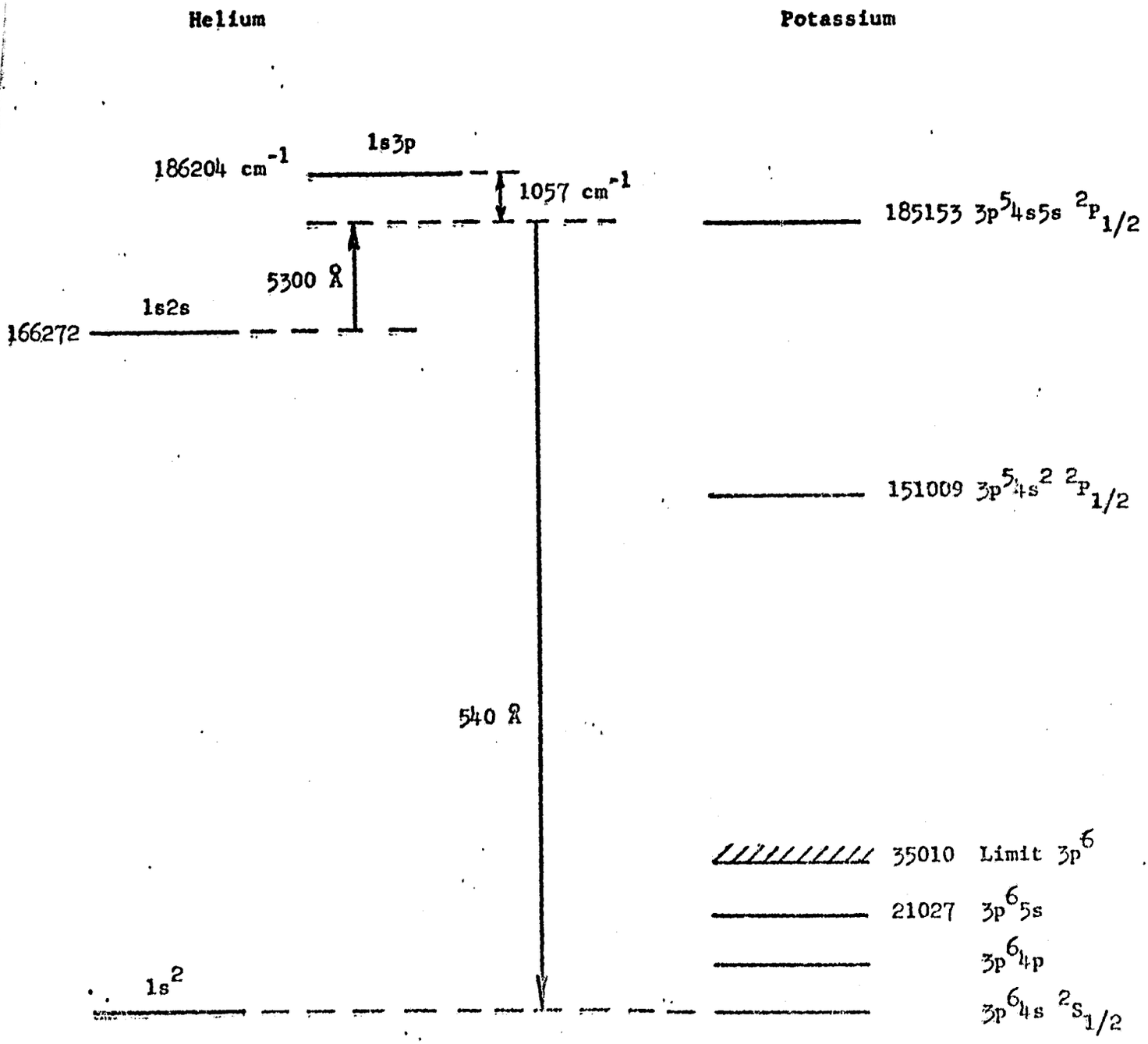

Fig. 3--Energy level diagram for spectroscopic studies of potassium autoionizing lines using the helium anti-Stokes VUV source.

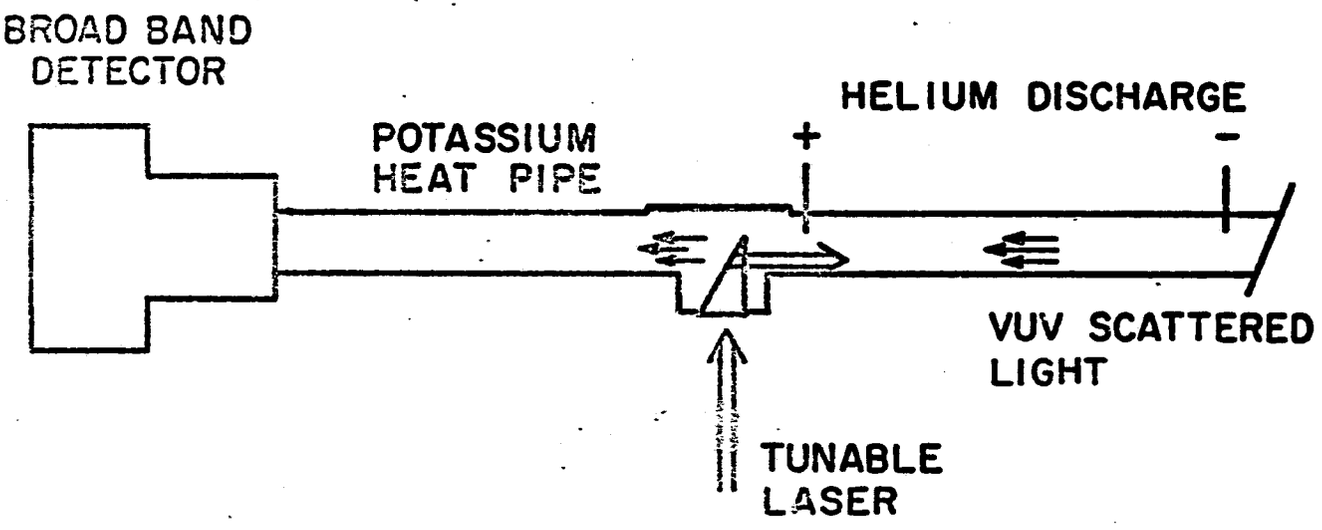

Fig. 4--VUV anti-Stokes spectroscopy in potassium.

one electron drops into the closed innershell and ionizes the other electron. We plan to investigate a number of autoionizing lines in K, as well as in other alkali metals.

We note that this source of tunable, intense, incoherent VUV light has a number of other possible applications: photolithographic fabrication of microstructures; the analysis of surface composition and properties, including catalytic surfaces; and the testing and evaluation of the compatibility of materials and components in a high VUV flux environment.

D. Generation and Applications of Ultrashort Optical Pulses

(A.E. Siegman and J-M. Heritier)

Satellite optical communications systems which are under development use mode-locked lasers to generate the very short, high repetition rate pulses needed for high data rates in optical links between satellites. In particular, the CW mode-locked Nd:YAG laser is a promising candidate for such space-borne communications systems. It is very desirable, however, to convert the near infrared oscillation wavelength of the YAG laser (1.064 microns) to its second harmonic in the green, in order to obtain both much better detector sensitivity and better beam collimation at the shorter wavelength. Because of the low power level involved in a CW mode-locked laser, especially in space-borne applications, doubling the laser pulses in the usual fashion with a nonlinear crystal outside the laser cavity cannot be done with adequate conversion efficiency. The solution is then to place the doubling crystal inside the laser cavity where the circulating optical pulse intensity is much larger; and in essence to use the harmonic conversion process as the output coupling from the YAG laser.

While this completely solves the harmonic conversion efficiency problem, the presence of a nonlinear doubling crystal inside the mode-locked laser can have serious negative effects on the laser mode-locking process, and can substantially broaden the mode-locked pulses in the laser. A reliable and detailed analysis of the pulse forming process in a laser which is simultaneously mode-locked and intracavity frequency doubled is thus important for optimizing the design and the understanding of such

lasers. During the past period we have completed such a detailed analysis that overcomes essentially all of the disadvantages associated with earlier treatments of this problem. Our work includes both computer studies and purely analytical results which provide new insight into this mode of operation, as well as providing detailed numerical results for all aspects of the laser performance in terms of the fundamental design parameters of the laser system. In addition to simplified analytical design formulas, a simplified but realistic physical description of the important detuning behavior of this laser is developed. Good agreement has been found between our analysis and experimental studies carried out in industrial laboratories. In particular, our analysis confirms that the mode-locked pulse width actually decreases as the modulation frequency is detuned off resonance; the harmonic power output initially increases for very small detuning, but then decreases; and the pulse shape develops a sharp edged asymmetry which is of opposite sense for opposite signs of detuning.

III. PUBLICATIONS RESULTING FROM THIS GRANT AND ITS PREDECESSOR

1. S. E. Harris, "Proposed Backward Wave Oscillation in the Infrared," Appl. Phys. Letters 9, 114 (August 1966).

2. S. E. Harris, "Stabilization and Modulation of Laser Oscillators by Internal Time-Varying Perturbation," Proc. IEEE 5, 10 (October 1966).

3. S. E. Harris, "Threshold of Multi-Mode Parametric Oscillators," IEEE J. Quant. Elect. QE-2, 701 (October 1966).

4. L. M. Osterink and R. Targ, "Single Frequency Light From an Argon FM Laser," Appl. Phys. Letters 10, 115 (February 1967).

5. O. P. McDuff and S. E. Harris, "Nonlinear Theory of the Internally Loss Modulated Laser," IEEE J. Quant. Elect. QE-3, 101 (March 1967).

6. S. E. Harris, M. K. Oshman, and R. L. Byer, "Observation of Tunable Optical Parametric Fluorescence," Phys. Rev. 18, 732 (May 1967).

7. L. M. Osterink, "The Argon Laser With Internal Phase Modulation — Its Use in Producing Single Frequency Light," Ph.D. Dissertation, Stanford University, Stanford, California (May 1967).

8. M. K. Oshman, "Studies of Optical Frequency Parametric Oscillation," Ph.D. Dissertation, Stanford University, Stanford, California (December 1967).

9. M. K. Oshman and S. E. Harris, "Theory of Optical Parametric Oscillation Internal to the Laser Cavity," IEEE J. Quant. Elect. QE-4, 491 (August 1968).

10. R. L. Byer, M. K. Oshman, J. F. Young, and S. E. Harris, "Visible CW Parametric Oscillator," Appl. Phys. Letters 13, 109 (August 1968).

11. R. L. Byer, "Parametric Fluorescence and Optical Parametric Oscillation," Ph.D. Dissertation, Stanford University, Stanford, California (December 1968).

12. S. E. Harris, "Nonlinear Optical Materials," Microwave Laboratory Report No. 1728, Stanford University, Stanford, California (March 1969).

13. Joel Falk and J. E. Murray, "Single Cavity Noncollinear Parametric Oscillation," Appl. Phys. Letters 14, 245 (April 1969).

14. S. E. Harris and R. W. Wallace, "Acousto-Optic Tunable Filter," J. Opt. Soc. Amer. 59, 744 (June 1969).

15. S. E. Harris, "Method to Lock an Optical Parametric Oscillator to an Atomic Transition," Appl. Phys. Letters 14, 335 (June 1969).

16. A. Kovrigin and R. L. Byer, "Stability Factor for Optical Parametric Oscillators," IEEE J. Quant. Elect. QE-5, 384 (July 1969).

17. R. L. Byer, A. Kovrigin, and J. F. Young, "A CW Ring-Cavity Parametric Oscillator," Appl. Phys. Letters 15, 136 (September 1969).

18. J. F. Young, "A Computer Program to Analyze Optical Resonators," Microwave Laboratory Report No. 1803, Stanford University, Stanford, California (November 1969).

19. S. E. Harris, "Tunable Optical Parametric Oscillator," Proc. IEEE 57, 2096 (December 1969).

20. J. E. Murray and S. E. Harris, "Pulse Lengthening Via Overcoupled Internal Field Harmonic Generation," J. Appl. Phys. 41, 609 (February 1970).

21. S. C. Wang, R. L. Byer, and A. E. Siegman, "Observation of an Enhanced Lamb Dip With a Pure Xe Gain Cell Inside a 3.51μ He-Xe Laser," Appl. Phys. Letters 17, 120 (August 1970).

22. S. C. Wang and A. E. Siegman, "Absorption Coefficient, Transition Probability, and Collision Broadening Frequency of Dimethylether at He-Xe Laser 3.51μ Wavelength," IEEE J. Quant. Elect. QE-6, 576 (September 1970).

23. William Streifer and John R. Whinnery, "Analysis of Dye Laser Tuned by Acousto-Optic Filter," Appl. Phys. Letters 17, 535 (October 1970).

24. J. F. Young, R. B. Miles, S. E. Harris, and R. W. Wallace, "Pump Linewidth Requirement for Optical Parametric Oscillators," J. Appl. Phys. 42, 497 (January 1971).

25. J. F. Young, J. E. Murray, R. B. Miles, and S. E. Harris, "Q-Switched Laser With Controllable Pulse Length," Appl. Phys. Letters 18, 129 (February 1971).

26. K. R. Manes and A. E. Siegman, "Observation of Quantum Phase Fluctuations in Infrared Gas Lasers," Phys. Rev. 4A, 373 (July 1971).

27. Helge Kildal and Robert L. Byer, "Monitoring Air Pollution," Laser Focus, p. 41 (October 1971).

28. D. J. Taylor, S. E. Harris, S. T. K. Nieh, and T. W. Hansch, "Electronic Tuning of a Dye Laser Using the Acousto-Optic Filter," Appl. Phys. Letters 19, 269 (October 1971).

29. D. J. Kuizenga, "Mode-Locking of the CW Dye Laser," Appl. Phys. Letters 19, 260 (October 1971).

30. H. Kildal and R. L. Byer, "Comparison of Laser Methods for the Remote Detection of Atmospheric Pollutants," Proc. IEEE 59, 1644 (December 1971).

31. J. F. Young, G. C. Bjorklund, A. H. Kung, R. B. Miles, and S. E. Harris, "Third Harmonic Generation in Phase Matched Rb Vapor," Phys. Rev. Letters 27, 1551 (December 1971).

32. A. E. Siegman and D. J. Kuizenga, "Laser Mode Locking Using Intracavity Modulators," Invited Paper, VIII International Quantum Electronics Conference, Montreal, Canada, May 8-11, 1972.

33. A. E. Siegman, "An Antiresonant Ring Interferometer for Coupled Laser Cavities, Laser Output Coupling, Mode Locking, and Cavity Dumping," IEEE J. Quant. Elect. QE-9, 247 (February 1973).

34. R. B. Miles and S. E. Harris, "Optical Third Harmonic Generation in Alkali Metal Vapors," IEEE J. Quant. Elect. QE-9, 470 (April 1973).

35. S. E. Harris, A. H. Kung, E. A. Stappaerts, and J. F. Young, "Stimulated Emission in Multiple Photon Pumped Xenon and Argon Excimers," Appl. Phys. Letters 23, 232 (September 1973).

36. D. J. Kuizenga, D. W. Phillion, T. Lund, and A. E. Siegman, "Simultaneous Q-Switching and Mode-Locking in the CW Nd:YAG Laser," Optics Comm. 9, 221 (November 1973).

37. S. E. Harris, J. F. Young, A. H. Kung, D. M. Bloom, and G. C. Bjorklund, "Generation of Ultraviolet and Vacuum Ultraviolet Radiation," in Laser Spectroscopy, R. G. Brewer and A. Mooradian, eds. (New York: Plenum Publishing Corp., 1974), p. 59.

38. A. E. Siegman and D. J. Kuizenga, "Active Mode-Coupling Phenomena in Pulsed and Continuous Lasers," Opto-Electronics 6, 43 (1974).

39. S. E. Harris and D. M. Bloom, "Resonantly Two-Photon Pumped Frequency Converter," Appl. Phys. Lett. 24, 229 (March 1974).

40. D. M. Bloom, James T. Yardley, J. F. Young, and S. E. Harris, "Infrared Up-Conversion With Resonantly Two-Photon Pumped Metal Vapors," Appl. Phys. Lett. 24, 427 (May 1974).

41. S. E. Harris, "Nonlinear Optical Techniques for Generation of VUV and Soft X-Ray Radiation," Proceedings of the Rank Prize Funds International Symposium on Very High Resolution Spectroscopy, London, England, September 1974.

42. G. C. Bjorklund, S. E. Harris, and J. F. Young, "Vacuum Ultraviolet Holography," Appl. Phys. Lett. 25, 451 (October 1974).

43. E. A. Stappaerts, "Harmonic Generation at High Field Strengths, Frequency Shifts and Saturation Phenomena," Phys. Rev. A 11, 1664 (May 1975).

44. D. M. Bloom, G. W. Bekkers, J. F. Young, and S. E. Harris, "Third Harmonic Generation in Phase Matched Alkali Metal Vapors," Appl. Phys. Lett. 26, 687 (June 1975).

45. D. M. Bloom, J. F. Young, and S. E. Harris, "Mixed Metal Vapor Phase Matching for Third Harmonic Generation," Appl. Phys. Lett. 27, 390 (October 1975).

46. Andre J. Duerinckx, "Pulse Compression in Mode-Locked Lasers Using Intracavity Self-Phase Modulation," J. Opt. Soc. Am. 66, 1076 (October 1976). [Abstract].

47. L. J. Zych and J. F. Young, "Limitation of 3547 Å to 1182 Å Conversion Efficiency in Xe," IEEE J. Quant. Elect. QE-14, 147 (March 1978).

48. W. R. Green and R. W. Falcone, "Inversion of the Resonance Line of Sr^+ Produced by Optically Pumping Sr Atoms," Optics Lett. 2, 115 (May 1978).

49. L. J. Zych, J. Lukasik, J. F. Young, and S. E. Harris, "Laser Induced Two-Photon Blackbody Radiation in the VUV," Phys. Rev. Lett. 40, 1493 (June 1978).

50. S. E. Harris, J. Lukasik, J. F. Young, and L. J. Zych, "Anti-Stokes Emission as a VUV and Soft X-Ray Source," in Picosecond Phenomena, C. V. Shank, E. P. Ippen, and S. L. Shapiro, eds. (New York: Springer-Verlag, 1978).

51. S. E. Harris and J. F. Young, "Rapid Laser Induced Energy Transfer in Atomic Systems," in Radiation Energy Conversion in Space, Kenneth W. Billman, ed. (New York: American Institute of Aeronautics and Astronautics, 1978).

52. Andre J. Duerinckx, Herman Vanherzeele, Jean-Louis Van Eck, and A. E. Siegman, "Pulse Compression Inside an Actively AM Mode-Locked Nd:YAG Laser Using a Liquid Kerr Cell," IEEE J. Quant. Elect. QE-14, 983 (December 1978).

53. A. E. Siegman and Jean-Marc Heritier, "Analysis of the Mode-Locked Intracavity Frequency-Doubled Nd:YAG Laser," IEEE J. Quant. Elect. QE-16, 324 (March 1980).

54. R. W. Falcone and G. A. Zdasiuk, "Pair Absorption Pumped Barium Laser," Optics Lett. 5, 155 (April 1980).

APPENDIX A

"Pair-Absorption-Pumped Barium Laser"

Pair-absorption-pumped barium laser

R. W. Falcone and G. A. Zdasiuk

Edward L. Ginzton Laboratory, Stanford University, Stanford, California 94305

Received November 11, 1979

This is the first reported demonstration of the use of pair-absorption transitions for optically pumping lasers. In a mixture of barium and thallium metal vapors, single-photon absorption of 3867-Å laser light caused simultaneous excitation of colliding ground-state atoms to the Ba($6s6p\ ^1P_1^\circ$) and Tl($6p\ ^2P_{3/2}^\circ$) excited states. Excited-state densities of about 10^{14} cm^{-3} were created, and subsequent laser emission on the Ba($6s6p\ ^1P_1^\circ$) → Ba($6s5d\ ^1D_2$) atomic transition at 1.5 μm was observed.

We describe the first reported demonstration of laser excitation of pair-absorption transitions as a technique for optically pumping new types of lasers. In particular, we have simultaneously excited colliding ground-state barium and thallium atoms to the Ba($6s6p\ ^1P_1^\circ$) and Tl($6p\ ^2P_{3/2}^\circ$) excited states by single-photon absorption of laser light at 3867 Å. Subsequent laser emission on the inverted Ba($6s6p\ ^1P_1^\circ$) → Ba($6s5d\ ^1D_2$) transition was observed at 1.5 μm.

Pair absorption, or simultaneous excitation, refers to a process in which two colliding atoms absorb a single photon at a wavelength corresponding to the sum energy of excited states of the individual species. After the collision the atoms separate, leaving both atoms in excited states. In the case of a dipole–dipole collisional interaction, one species makes a (dipole) allowed transition while the other species makes a (dipole) nonallowed transition. The use of laser excitation of pair-absorption transitions for pumping new types of lasers was proposed in Ref. 1. The pair-absorption process is a specific example of a general class of reactions now called laser-induced collisions.[2,3] Pair absorption has recently been observed in atomic-metal vapors in the visible spectrum[4]; previously it had been observed in molecular systems in the infrared.[5]

We have studied the pair-absorption process

$$\mathrm{Ba}(6s^2\ ^1S_0) + \mathrm{Tl}(6p\ ^2P_{1/2}^\circ) + \hbar\omega_p(3867\ \text{Å}) \rightarrow \mathrm{Ba}(6s6p\ ^1P_1^\circ) + \mathrm{Tl}(6p\ ^2P_{3/2}^\circ). \quad (1)$$

As shown in Fig. 1, the Ba atom is excited on an allowed transition and the Tl atom is excited on a nonallowed transition. The absorption process of Eq. (1) maximizes when the photon energy, $\hbar\omega_p$, is equal to the sum of the energies of the atomic excited-state products.

The absorption coefficient for pair absorption, $\alpha(\mathrm{cm}^{-1})$, is given on line center by

$$\alpha = \frac{8e^6\omega_p f_1 f_2 f_3[\mathrm{Tl}^\circ][\mathrm{Ba}^\circ]}{m^3 c\bar{V}\rho^2(\Delta\omega)^2\omega_1\omega_2\omega_3}, \quad (2)$$

where e is the electronic charge; $\omega_p = 2\pi c/\lambda_p$ is the angular frequency of the absorbed light; f_1, f_2, f_3 and ω_1, ω_2, ω_3 are the oscillator strengths and frequencies of the atomic transitions Tl($6p\ ^2P_{1/2}^\circ$) → Tl($7s\ ^2S_{1/2}$), Tl($7s\ ^2S_{1/2}$) → Tl($6p\ ^2P_{3/2}^\circ$), and Ba($6s^2\ ^1S_0$) → Ba($6s6p\ ^1P_1^\circ$), respectively; [Tl°] and [Ba°] are the ground-state number densities of the colliding atoms; m is the electron mass; c is the velocity of light; $\bar{V}$ is the relative velocity of the colliding atoms; ρ is the Weisskopf radius[6] or dephasing radius of the collision (11 Å in this experiment); and $\Delta\omega$ is the frequency detuning of the pump laser relative to the atomic transition in Tl, as indicated in Fig. 1. Equation (2) was derived by using perturbation theory as detailed in the treatment of laser-induced collisional processes given in Ref. 7. The excited-state densities of both species, Ba*($6s6p\ ^1P_1^\circ$) and Tl*($6p\ ^2P_{3/2}^\circ$), are given by

$$[\mathrm{Ba}^*] = [\mathrm{Tl}^*] = \frac{P/A}{\hbar\omega_p}\alpha\tau_p, \quad (3)$$

where P/A is the power density and τ_p is the pulse length of the applied laser.

An experimental schematic is shown in Fig. 2. The 3867-Å radiation was produced by sum-frequency generation in KD*P of 6075-Å and 1.06-μm laser light by using a Quanta Ray Nd:YAG dye-laser system; pulse energies at 3867 Å of up to 5 mJ in a 5-nsec pulse were available. This beam was collimated to a spot size of 0.15 cm^2 and directed into a metal-vapor oven containing Ba and Tl heated to 1400°C over a vapor-zone length of 10 cm. The cell also contained ~250 Torr of argon gas to prevent metal-vapor diffusion and con-

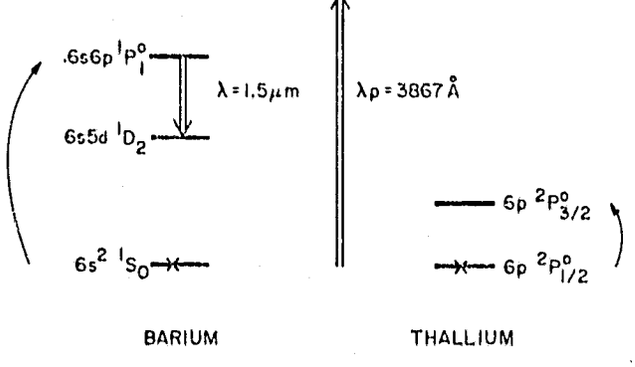

Fig. 1. Barium and thallium energy levels for the pair-absorption-pumped atomic barium laser.

Reprinted from Optics Letters, Vol. 5, No. 4, page 155, April, 1980

densation on the cold cell windows. The 1.5-μm output light from the cell was filtered with a spectrometer and detected with a room-temperature InSb detector.

Figure 3 shows an absorption scan of the metal-vapor cell in the region of pair absorption made by using a continuum discharge lamp. The shape of the curve agrees with the data of Ref. 4. A curve-of-growth analysis of the resonance-line absorptions of Ba and Tl yielded ground-state vapor densities of $[Ba^\circ] = 4 \times 10^{17}$ cm^{-3} and $[Tl^\circ] = 2 \times 10^{17}$ cm^{-3} in the cell. The measured absorption at 3867 Å was 35%, compared with the predicted value of 80% at these densities using Eq. (2). This discrepancy is most probably due to uncertainties in our measurement of the ground-state number densities.

When the pump laser was tuned to 3867 Å, laser emission at 1.5000 ± 0.0001 μm, corresponding to the Ba($6s6p\ ^1P_1^\circ$) → Ba($6s5d\ ^1D_2$) transition,[8] was observed. The emission was narrow band (less than 0.2-Å spectrometer resolution) and exhibited threshold behavior at a pump energy of 1 mJ. Spatial collimation was verified by placing a variable aperture between the detector and the cell. As the pump wavelength was tuned about 3867 Å, the observed emission wavelength at 1.5 μm remained constant. Our measurement of the duration of the 1.5-μm emission was limited by the response time of the InSb detector to <100 nsec. [The spontaneous decay time of the Ba($6s6p\ ^1P_1^\circ$) → Ba($6s5d\ ^1D_2$) transition is ~200 nsec.[8]] The intensity of the emission as a function of pump-laser wavelength is shown in Fig. 4. The intensity maximizes at a pump wavelength of 3867 Å, and the profile has an asymmetry to longer wavelengths that is also seen on the absorption scan in Fig. 3. This asymmetry is predicted from a consideration of the interaction potentials[4] of the colliding atoms.

The bandwidth of the pair absorption is about 1 Å (7 cm^{-1}). This absorption linewidth is characteristic of light-induced collision processes[2] and is independent of both metal-vapor density (in the linear absorption regime) and buffer-gas density.

The measured cell absorption of 35% at 3867 Å implies an optically pumped excited-state density of Ba($6s6p\ ^1P_1^\circ$) of about 5×10^{14} cm^{-3} at the lasing threshold pump energy of 1 mJ per pulse. This estimated excited-state density is consistent with calculations of the required threshold excited-state density, allowing for the 1×10^{14} cm^{-3} thermal population of the lower laser level.

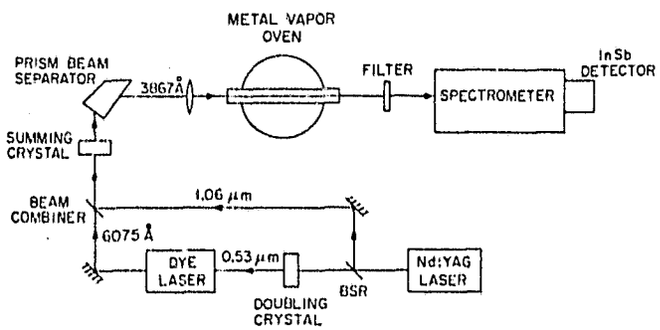

Fig. 2. Experimental schematic.

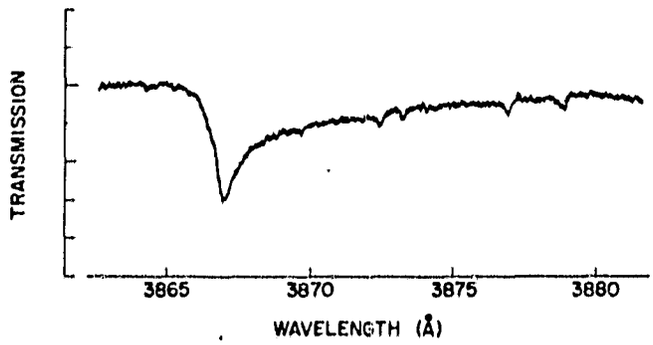

Fig. 3. Absorption scan showing barium–thallium pair absorption at 3867 Å.

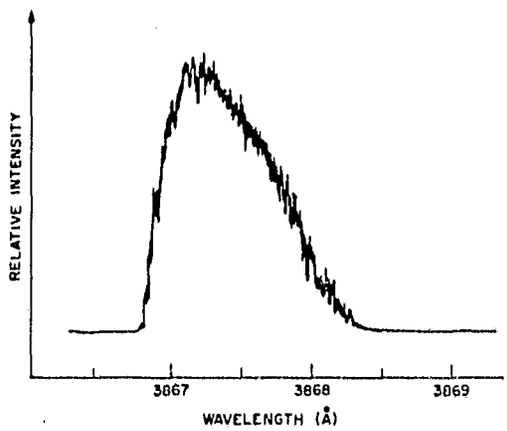

Fig. 4. Relative intensity of the $\lambda = 1.5$ μm atomic barium laser as a function of pumping wavelength.

This experiment demonstrates a new technique for optically pumping high densities of atomic (and molecular) species using the relatively large-bandwidth cross section of pair-absorption transitions. One of the most promising aspects of this technique is that new absorption wavelengths are created by mixing different species together; this provides a method for channeling the energy of high-powered, fixed-wavelength lasers into specific target states of atoms that otherwise would not absorb the radiation.

A further possible application of this technique is the use of pair absorption for the inversion of atoms and molecules to the ground state, as pointed out in Ref. 1. A high density of one species will permit the inversion of the second species to the ground state when sufficient pump-laser energy is applied at the pair-absorption wavelength. One application of this technique would be the temporal and spectral compression of high-powered excimer lasers. The energy stored in the inverted species by optical pumping with the excimer laser could be rapidly extracted in a narrow-bandwidth pulse by Raman, two-photon, or another lasing process to the emptied ground state.

We wish to thank S. E. Harris and J. F. Young for helpful discussions.

This research was supported jointly by the National Aeronautics and Space Administration under Contract NGL-05-020-103 and the U.S. Air Force under Contract F19628-77-C-0072.

References

1. R. W. Falcone, Appl. Phys. Lett. 34, 150 (1979).
2. S. E. Harris, J. F. Young, W. R. Green, R. W. Falcone, J. Lukasik, J. C. White, J. R. Willison, M. D. Wright, and G. A. Zdasiuk, in *Laser Spectroscopy IV*, H. Walther and K. W. Rothe, eds. (Springer-Verlag, New York, 1979).
3. L. I. Gudzenko and S. I. Yakovlenko, Phys. Lett. A 46, 475 (1974).
4. J. C. White, G. A. Zdasiuk, J. F. Young, and S. E. Harris, Opt. Lett. 4, 137 (1979).
5. H. L. Welsh, M. F. Crawford, J. C. F. MacDonald, and O. A. Chisholm, Phys. Rev. 83, 1264 (1951).
6. W. R. Hindmarsh and J. M. Farr, *Collision Broadening of Spectral Lines by Neutral Atoms* (Pergamon, Oxford, 1972).
7. S. E. Harris and J. C. White, IEEE J. Quantum Electron. **QE-13**, 972 (1977).
8. B. M. Miles and W. L. Wiese, "Critically evaluated transition probabilities for Ba I and II," NBS Tech. Note No. 474 (U.S. Government Printing Office, Washington, D.C., 1969).

APPENDIX B

"Analysis of Mode-Locked and Intracavity Frequency-Doubled Nd:YAG Laser"

Analysis of Mode-Locked and Intracavity Frequency-Doubled Nd:YAG Laser

A. E. SIEGMAN, FELLOW, IEEE, AND JEAN-MARC HERITIER

Abstract—We present analytical and computer studies of the CW mode-locked and intracavity frequency-doubled Nd:YAG laser which provide new insight into the operation, including the detuning behavior, of this type of laser. Computer solutions show that the steady-state pulse shape for this laser is much closer to a truncated cosine than to a Gaussian; there is little spectral broadening for on-resonance operation; and the chirp is negligible. This leads to a simplified analytical model carried out entirely in the time domain, with atomic linewidth effects ignored. Simple analytical results for on-resonance pulse shape, pulse width, signal intensity, and harmonic conversion efficiency in terms of basic laser parameters are derived from this model. A simplified physical description of the detuning behavior is also developed. Agreement is found with experimental studies showing that the pulsewidth decreases as the modulation frequency is detuned off resonance; the harmonic power output initially increases and then decreases; and the pulse shape develops a sharp-edged asymmetry of opposite sense for opposite signs of detuning.

I. Introduction

THE CW mode-locked Nd:YAG laser provides a reasonably efficient, reliable, and well-engineered source of optical pulses with high repetition rates (~500 MHz), narrow pulsewidths (≤100 ps), and moderate powers (~1 W average). The Nd:YAG wavelength of 1.064 μm is, however, further into the IR than is desirable for some applications, and the peak pulse intensity in the output beam is too low to permit efficient second-harmonic generation outside the cavity.

A possible approach is then to employ intracavity second-harmonic generation (SHG), with the harmonic crystal placed inside the laser cavity. The harmonic conversion efficiency is substantially increased because of the larger fundamental intensity circulating inside the laser cavity, and at the same time only small conversion is required because the harmonic conversion efficiency need only equal the usual output coupling per pass from the laser (typically ≤10 percent) to efficiently extract most of the available fundamental power at the second-harmonic wavelength.

This type of laser can be important in satellite optical communications systems, laser radars, and other applications, and several previous studies of this mode of operation have been published [1]-[9]. In general, the intracavity harmonic-generation and mode-locking processes are found to be in opposition, with the harmonic-generation process producing a "peak-clipping" effect which substantially broadens the mode-locked pulses. In addition, the laser performance is found to be extremely sensitive to small detunings between the active mode-locking modulation frequency and the actual roundtrip transit time in the laser.

Previous analyses of the mode-locked and frequency-doubled laser [4]-[8] have used approximations such as assuming a Gaussian mode-locked pulse shape and then manipulating the parameters of the Gaussian pulse to obtain a self-consistent steady-state situation. It will become apparent from this paper that a Gaussian pulse is not an adequate approximation for the actual pulse shape in a mode-locked and frequency-doubled laser (as was in fact noted much earlier [4]). Previous analyses have also generally established only indirect connections between basic laser parameters and the resulting mode-locked laser performance, and have in general not explored the important detuning behavior.

In this paper, we present both "exact" computer calculations and new analytical results describing the performance of a typical CW mode-locked Nd:YAG laser with intracavity SHG, including detuning effects. Insights provided by the computer results enable us to develop simple analytic expressions which give the mode-locked pulse shape, pulsewidth, power output, and harmonic conversion efficiency for zero detuning directly in terms of the basic design parameters of this type of laser. We also develop a physical picture and analytical results for the detuning behavior of the laser in response to small changes in modulation frequency or cavity length. These results appear to be in good agreement with such experimental results as are available.

In the remainder of the paper, Section II briefly reviews the basic analytical model, while Section III presents exact computer solutions based on that model. Section IV then develops a simplified form of the analytical model for zero detuning, leading to simple analytical expressions for all the basic on-resonance performance characteristics of the system. These expressions are also expanded into greater detail in the Appendix. Finally, Section V gives further results for the detuning behavior of the laser, based on the simplified analytical model.

The work described here was first motivated by experimental results obtained by D. Radecki and A. Kramer at GTE Sylvania [9]. The agreement between these analytical and experimental results is found to be quite good.

II. Analytical Model

A. Laser Pulse Parameters

We employ the same analytical model used in earlier analyses [4]-[7], as illustrated in Fig. 1. We consider a fundamental-frequency optical pulse circulating inside the laser cavity of the form

Manuscript received August 15, 1979. This work was supported by NASA under Contract NGL-05-020-103 and Grant NSG-7619.

A. E. Siegman is with the Department of Electrical Engineering and the Edward Ginzton Laboratory, Stanford University, Stanford, CA 94305.

J.-M. Heritier is with the Department of Applied Physics, Stanford University, Stanford, CA 94305.

0018-9197/80/0300-0324$00.75

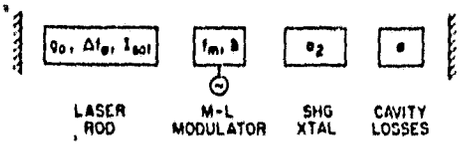

Fig. 1. Analytical model for the mode-locked and internally frequency-doubled laser.

$$\mathcal{E}_1(t) = \mathrm{Re}\, E_1(t)\, e^{j2\pi f_0 t} \tag{1}$$

where $E_1(t)$ is the complex phasor amplitude and f_0 is the center frequency of the atomic line. For simplicity, the field amplitude is normalized so that the instantaneous intensity (power/unit area) in the pulse is

$$I_1(t) = |E_1(t)|^2. \tag{2}$$

Similar expressions with subscript 2 and frequency $2f_0$ represent the second-harmonic quantities. The pulse amplitude spectrum, or the complex frequency transform of $\mathcal{E}_1(t)$, is written as $\mathcal{E}_1(f) = E_1(f - f_0)$, so that $E_1(f)$ is the Fourier transform of the pulse envelope $E_1(t)$. We write the transforms using hertzian frequencies f rather than radian frequencies $\omega = 2\pi f$ because this matches more naturally the discrete Fourier transforms used in the computer calculations.

The single pulse energies per unit area at the fundamental and harmonic frequencies inside the laser cavity are given by

$$W_1 = \int I_1(t)\, dt$$

$$W_2 = \int I_2(t)\, dt \tag{3}$$

where the integrals are over one period of the mode-locking frequency. It is assumed that the second-harmonic power will be efficiently coupled out of the laser cavity by an appropriate dichroic mirror, so that W_2 also represents the second-harmonic output energy per pulse per unit beam area.

B. Gain Medium

Following earlier analyses [5], [7], the one-way or single-pass voltage gain through the homogeneous laser medium and once down the laser cavity of length L is given by the Lorentzian gain expression

$$T_A(f) = \exp\left[\frac{g}{1 + 2j(f - f_0)/\Delta f_a} - j2\pi f L/c\right] \tag{4}$$

where g is the saturated one-way voltage gain coefficient in the laser medium and Δf_a is the FWHM atomic linewidth (~120–150 GHz in Nd:YAG). In the lasers of interest here, the pulse repetition rate is much higher than the inverse relaxation time of the laser medium. Hence, the laser gain saturates homogeneously on the average rather than the instantaneous circulating power in the form

$$g = \frac{g_0}{1 + 2W_1/W_{\mathrm{sat}}} \tag{5}$$

where g_0 is the unsaturated single-pass voltage gain coefficient. The saturation energy W_{sat} (per unit area and per pulse) is related to the usual saturation intensity I_{sat} of the laser medium by

$$W_{\mathrm{sat}} = T_m I_{\mathrm{sat}} = I_{\mathrm{sat}}/f_m \tag{6}$$

where the modulation frequency $f_m \equiv T_m^{-1}$ is the repetition frequency of the mode-locked laser pulses, and is typically several hundred megahertz. The factor of two appears in (5) because the laser medium is saturated by the circulating power going in both directions inside the cavity.

C. Modulator

The single-pass amplitude transfer function through the AM mode-locking modulator, together with the linear cavity losses, is given by [4]

$$T_m(t) = \exp\left[-\alpha - \delta \sin^2(\pi f_m t)\right] \tag{7}$$

where α is the single-pass voltage loss coefficient due to ohmic losses, scattering, mirror-outcoupling, and any other linear cavity loss mechanisms, and δ is the AM modulation index.

D. Nonlinear Crystal

The roundtrip or double-pass harmonic conversion in the SHG crystal is defined by the instantaneous relationship

$$I_2(t) = 2a_2 I_1^2(t) \tag{8}$$

where $I_1(t)$ is the circulating instantaneous fundamental intensity in the cavity; $I_2(t)$ is the instantaneous second-harmonic intensity generated after a complete double pass through the SHG crystal; and a_2 is an effective nonlinearity coefficient for the SHG crystal. For small fractional conversion and weak focusing in the SHG crystal, this parameter is given in practical terms (and MKS units) by

$$2a_2 \approx 2M\omega_0^2\, d^2 (\mu/\epsilon)^{3/2}\, \mathrm{sinc}^2(\Delta k l/2) \tag{9}$$

where $2d$ is the ratio of instantaneous nonlinear polarization to instantaneous electric field in the nonlinear material; M is the ratio of beam cross-section area in the laser rod to the same quantity in the SHG crystal, as controlled by the cavity optics; Δk is the phase mismatch between waves at ω_0 and $2\omega_0$; l is the total effective interaction length in the nonlinear crystal, which can range up to twice the physical crystal length if the crystal is double passed with proper phasing between passes; and $\mathrm{sinc}\, x \equiv (\sin x)/x$. As long as the fractional harmonic conversion per pass is small (which will always be the case in practice), the double-pass amplitude transmission of the nonlinear crystal for the fundamental frequency can be expressed by

$$\mathcal{E}_1'(t) = \mathcal{E}_1(t)\left[1 - a_2 |\mathcal{E}_1(t)|^2\right] = \mathcal{E}_1(t)\left[1 - a_2 I_1(t)\right] \tag{10}$$

where $\mathcal{E}_1'(t)$ is the value after the SHG crystal.

E. Detuning Parameter

The detuning behavior of the actively mode-locked laser is of particular importance. The (small) frequency difference f_d between the externally driven modulation frequency f_m and the $c/2L$ axial mode spacing of the empty laser cavity may be defined as

$$f_d \equiv (c/2L) - f_m. \tag{11}$$

This expression considers only the "cold" cavity repetition frequency $c/2L$ and does not take into account the frequency shift or added time delay contributed by the linear dispersion of the laser transition itself. From (4), the linear portion of the overall roundtrip cavity phase delay versus frequency at midband will be 0 when the modulation frequency is given by

$$f_m = \frac{c}{2L} - \frac{2gf_m^2}{\pi\Delta f_a}. \tag{12}$$

This occurs when the frequency difference of (11) has the value

$$f_d = f_{d0} \equiv \frac{2gf_m^2}{\pi\Delta f_a}. \tag{13}$$

The situation $f_d = f_{d0}$ is thus what one would call the "zero-detuning" condition, or the condition in which the modulation frequency f_m exactly matches the loaded roundtrip transit time, including the dispersive effect of the laser transition. The value of f_{d0}, however, depends on the saturated gain g of the laser medium, and this depends in turn on the circulating power, SHG nonlinearity, modulation depth, and other operating parameters. Thus, there does not exist any unique zero-detuning point for a mode-locked laser, independent of the actual operating conditions of the laser. One can estimate f_{d0} by knowing approximately the usual saturated gain in the laser. For the cases analysed in this paper, f_{d0} has a value around 15 kHz.

Note that the differential relationship between modulation frequency f_m and cavity length L is given by

$$\frac{\delta f_m}{\delta L} = -\frac{f_m}{L} \approx -1.67 \text{ kHz}/\mu\text{m} \tag{14}$$

for a cavity with $L = 30$ cm and $f_m = 500$ MHz. A value of $f_{d0} \approx 15$ kHz thus indicates that the atomic dispersion makes the cavity seem to be $\sim 9\,\mu$m longer than its cold electrical length. Changes in the physical cavity length of as little as $\pm 10\,\mu$m can cause significant detuning effects.

F. Available Energy and Power Output

If the same laser medium as above is operated CW (i.e., with both mode locking and SHG turned off), with the same unsaturated gain g_0 and loss α, and with an output mirror having power reflection factor $R = e^{-\delta_e} \approx 1 - \delta_e$, then the CW output intensity (W/unit area) at the fundamental frequency will be

$$I_{\text{out}} = \frac{\delta_e I_{\text{sat}}}{2}\left[\frac{4g_0}{4\alpha + \delta_e} - 1\right]. \tag{15}$$

For optimum output coupling given by $\delta_e = 4\alpha[(g_0/\alpha)^{1/2} - 1]$, the maximum available fundamental output intensity will be

$$I_{\max} = 2g_0[1 - (\alpha/g_0)^{1/2}]^2 I_{\text{sat}}. \tag{16}$$

This can be viewed as representing a maximum available power per unit area that can be extracted from the laser medium, namely $2g_0 I_{\text{sat}}$, reduced by an internal cavity loss factor $[1 - (\alpha/g_0)^{1/2}]^2$. Hence, there will be a maximum available energy per unit area, per pulse, that can be extracted from the laser medium in the mode-locked and doubled laser at the fundamental plus harmonic frequencies. A figure of merit for the laser is then how close the second-harmonic energy per pulse W_2 approaches this available pulse energy, taking into account also the internal cavity loss factors. We therefore define the second-harmonic extraction efficiency as

$$\eta_2 \equiv \frac{W_2}{2g_0[1 - (\alpha/g_0)^{1/2}]^2 W_{\text{sat}}}. \tag{17}$$

We will see later that η_2 has a maximum value of around 80 percent [4], [8] for the mode-locked and frequency-doubled laser.

G. Connection with Real Lasers

The analysis up to this point has been formulated entirely in terms of per-unit-area wave intensities. A rigorous analysis of the gain, saturation effects, and harmonic conversion processes inside a real laser of this type, taking into account the Gaussian transverse mode profile with spot size w, would be very much more complicated. To a good approximation, however, the second-harmonic power generated inside such a real laser can be related to the harmonic energy per pulse per unit area by

$$P_2 = A_{\text{eff}} f_m W_2 \tag{18}$$

where

$$A_{\text{eff}} \approx \pi w^2 \tag{19}$$

is an effective cross-section area for the laser beam inside the laser rod. The useful output power at the second harmonic may be reduced below this value by a coupling factor ≤ 1, in order to represent output coupler losses and other effects which may keep some of the harmonically generated power from being extracted out of the cavity. The circulating fundamental power P_1 can also be related to the fundamental energy per pulse W_1 by the same area A_{eff} without any coupling efficiency factor.

In making the connection between a real laser and the plane-wave theory, the effective area A_{eff}, the effective saturation intensity I_{sat}, and the effective harmonic conversion factor a_2, can all be regarded as adjustable parameters which may have to be adjusted slightly from their ideal or plane-wave values in order to take into account averaging effects across the Gaussian beam profile. To first order, this will have little effect on the predicted pulse shape, the pulsewidth, or the overall dependence on other laser parameters predicted by the present analysis.

III. Computer Solutions

Because of the difficulty in obtaining accurate analytical solutions for the mode-locked and frequency-doubled laser, we initially approached the problem by carrying out brute-force computer calculations, attempting to find more or less "exact" steady-state solutions to the analytical model of Section II. In essence, we propagated pulses repeatedly around the laser cavity by numerical simulation and observed the evolution of the pulse after repeated roundtrips. The results of these computer simulations are summarized in this section.

A. Simulation Procedure

To perform the calculations, we replaced the fundamental pulse envelope $E(t)$ during one period of the modulation cycle $-T_m/2 \leq t \leq T_m/2$ by N discrete sampled values $E_n \equiv W_{sat}^{-1/2} E(t_n)$ where $t_n = n\Delta t$ for $n = -(N/2)+1$ to $(N/2)$, and $\Delta t = T_m/N = 1/Nf_m$. The pulse spectrum $E(f - f_0)$ was similarly replaced by the discrete spectrum $E_n \equiv W_{sat}^{-1/2} E(f_n - f_0)$, where the frequency components $f_n = f_0 + nf_m$ correspond to the modulation sidebands of the periodically repeated pulse with n running over the same range. (Scaling the pulse amplitude to $W_{sat}^{-1/2}$ is merely a computational convenience.) Note that $n = 0$ corresponds to the peak or midpoint of the modulation cycle and also to the center of the atomic line in the frequency domain. With this notation, the pulse sample value E_n can be efficiently transformed back and forth between the time and frequency domains using the fast Fourier transform algorithm [10], [11]. Depending on circumstances, from $N = 64$ to $N = 1024$ discrete samples were employed.

The straightforward simulation procedure was then as follows. An arbitrary initial pulse E_n in the time domain (for example, a pulse with an initially uniform amplitude through the full modulation cycle) was stored in the data array; transformed (in place) into the frequency domain; and then multiplied by the discrete double-pass version of the complex amplifier-cavity transfer function, namely

$$T_A^2(f_n) = \exp\left[\frac{2g}{1 + 2j(f_m/\Delta f_a)\,n} + j2\pi(f_d/f_m)\,n\right]. \quad (20)$$

A suitable initial value of the gain $2g$ was used to start the calculation. The amplified pulse spectrum was then inverse transformed back to the time domain (call this result E_n') and double passed through the modulator and SHG crystal by calculating

$$E_n'' = T_M^2(t_n)[1 - a_2 W_{sat}|E_n'|^2]\,E_n' \quad (21)$$

where the modulator double-pass transmission is

$$T_M^2(t_n) = \exp\left[-2\alpha - 2\delta \sin^2(n\pi f_m \Delta t)\right]. \quad (22)$$

This computer simulation of one roundtrip was then repeated some number of times, typically 10–20, after which the total pulse energy and other pulse parameters were computed and stored. A new saturated gain value was then computed from (5), and using this new value of g the amplifier gain function (20) was recalculated and another 10–20 roundtrips carried out in a repeated cycle. This process was continued for as many as several thousand roundtrips for each set of basic laser parameters.

B. Windowing

A discrete simulation carried out using discrete Fourier transforms actually represents a model in which the discrete pulse samples are periodically repeated in both the time domain and the frequency domain. To avoid the well known aliasing effects that arise in this situation [10], [11], both the time and frequency transfer functions $T_A(f_n)$ and $T_M(t_n)$ were also multiplied by a window function given by

$$W(n) = \exp\left[-1.2(2n/N)^{16}\right]. \quad (23)$$

This more or less arbitrarily chosen window function smoothed out high-frequency ripples in the computer pulses and their spectra without materially altering the overall pulses. Mode-locked laser pulses are known to be very sensitive to the curvatures of the time and frequency domain transfer functions $T_A(f)$ and $T_M(t)$ near $f = f_0$ and $t = 0$. Therefore, the use of a window function like (23) with zero low-order derivatives at the center is important. Other more standard window functions [12] which have significant curvature near $n = 0$ were also tried but were observed to distort the computed pulses.

C. Numerical Parameters

These simulations were carried out primarily for a set of laser parameters similar to those of a typical laser system planned for a space-borne communications system [9], namely

Unsaturated single-pass power gain = $2g_0 = 0.03$
Single-pass power loss = $2\alpha = 0.007$
Modulation frequency = $f_m = 500$ MHz
Modulation depth = $2\delta = 0.08$
Atomic linewidth = $\Delta f_a = 120$ GHz
Nonlinearity coefficient = $a_2 W_{sat} = 4 \times 10^{-11}$ s.

Preliminary calculations showed that the saturated gain corresponding to these parameters was typically $2g \approx 0.023$. The zero-detuning value corresponding to this standard gain value is

$$f_{d0} = \frac{2gf_m^2}{\pi \Delta f_a} \approx 15\,250 \text{ Hz}. \quad (24)$$

Therefore, we tentatively establish the value $f_d \approx 15\,000$ Hz as the "zero-detuning" point in these calculations.

Note that the steady-state mode-locked pulsewidth τ_p given by the Kuizenga–Siegman model [13] without doubling would be

$$\tau_p = \left(\frac{4 \ln 2}{\pi^2}\right)^{1/2} \left(\frac{g_0}{\delta}\right)^{1/4} \left(\frac{1}{f_m \Delta f_a}\right)^{1/2} \approx 55 \text{ ps}. \quad (25)$$

The transform-limited spectral width (FWHM) corresponding to this pulsewidth would be ~7.5 GHz, or ~15 modulation sidebands. We will argue later that for pulsewidths substantially larger, or spectral widths substantially smaller, than these values the atomic lineshape must be playing only a minor role in the pulse-shaping process.

D. Computer Results with Zero Detuning

Fig. 2 shows a typical result of these computer calculations, including the fully converged fundamental pulse E-field envelope amplitude, the fundamental amplitude spectrum, and the second-harmonic pulse shape (pulse power), for the near-zero-detuning case after a large number of passes starting from a uniform input pulse. Essentially, the same converged solution was obtained with various initial conditions, and using as few as $N = 16$ sample points. For the value of $a_2 W_{sat} = 4 \times 10^{-11}$ s, which is not far from optimum, the fundamental pulsewidth (FWHM) is $\tau_{p1} = 405$ ps and the second-harmonic pulsewidth is $\tau_{p2} = 315$ ps, both of which are much larger than the value for the same laser and modulator without intra-

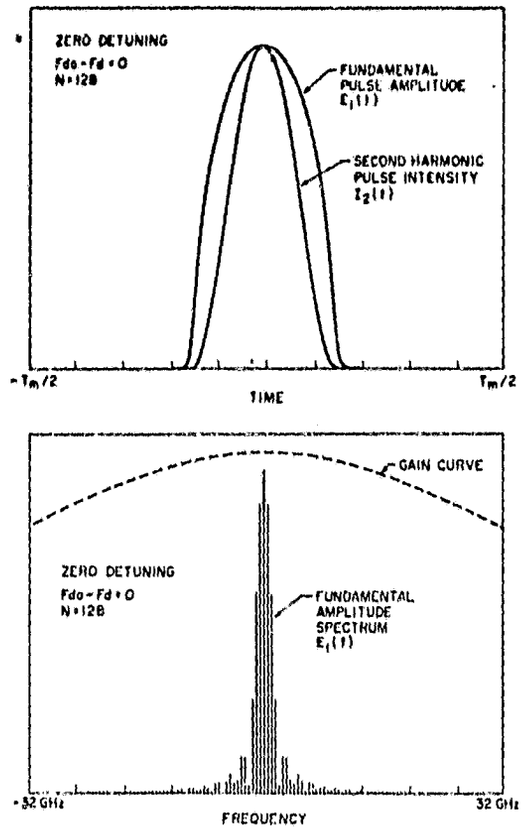

Fig. 2. Example of a fully converged steady-state pulse obtained from the computer simulation of the mode-locked and frequency-doubled laser under conditions of near-zero detuning and near-optimum harmonic coupling. The curves show the fundamental pulse field amplitude $E_1(t)$; the second-harmonic pulse intensity $I_2(t)$; the fundamental amplitude spectrum $E_1(f)$; and the Nd:YAG gain curve $|T_a(f)|$. The nonlinearity value used for the figure is $a_2 W_{sat} = 4 \times 10^{-11}$ s.

cavity doubling. The pulse spectrum correspondingly remains very narrow, and examination of the phase of the complex pulse envelope shows no evidence of "chirping" [14].

The internal harmonic conversion efficiency (average SHG power generated over average circulating fundamental power) is $\alpha_{SHG} \equiv W_2/W_1 \approx 2$ percent; and the second-harmonic extraction efficiency is $\eta_2 \approx 45$ percent. The mode-locked and frequency-doubled laser does a reasonably good job of extracting the available energy in the laser rod. However, it is clear that the mode-locked pulse shapes are far from Gaussian.

During the evolution of the numerical simulation process from an arbitrary initial pulse shape toward convergence, we observed that for zero detuning the fundamental pulse shape and pulse spectrum converged to essentially their final forms fairly quickly. However, the fundamental circulating power, the second-harmonic power, and the exact pulsewidth all continued to drift very slowly toward their final values even after a very large number (>1000) of roundtrips. This characteristic of the calculations (and presumably of the real laser also) apparently results from a delicate balance between the small and competing gain and loss mechanisms in the laser. For finite detuning the pulse calculations converged even more slowly, which represented a serious difficulty in performing a large number of such calculations. Whether the final convergence of these calculations could be significantly accelerated by more sophisticated numerical methods is not clear.

E. Computer Results with Finite Detuning

Experimental results obtained by Radecki and Kramer at GTE Sylvania [9] show that, for small but finite detuning of either the laser modulation frequency f_m or the cavity length L, the pulsewidth narrows; the circulating power and the second-harmonic output increase at first, and then decrease; and the pulse develops a steep asymmetric edge on one side of the pulse. Fig. 3 shows by way of comparison the computed pulse envelopes and spectra for three different values of $f_d = 0$ Hz, -15 000 Hz, and -65 000 Hz after 10 000, 15 000, and 38 000 roundtrips using $N = 128$, 512, and 512 points, respectively, all starting from the same initial pulse shape. The initial pulse shape in each case was the zero-detuning pulse shape of Fig. 2. The development of a sharp asymmetric leading edge on the detuned pulse envelopes and a broad pedestal on the pulse spectra is evident. The experimentally observed decrease in pulsewidth and increase in harmonic output with detuning is also at least qualitatively matched by these calculations.

Similar but less extensive calculations were carried out using detunings of $f_d = 15\,000$, 0, -15 000, -30 000, and +60 000 Hz. These results showed the same general features and in particular the $f_d = +60\,000$ Hz case showed essentially the same results as the $f_d = -30\,000$ Hz case except for a symmetric inversion of pulse shape about the pulse center, indicating that the zero-detuning value of $f_{d0} \approx 15\,000$ Hz is reasonable. The broad pedestal in the pulse spectrum developed sufficient breadth in these calculations, however, to indicate that a sizable number of sidebands must be included in the simulation; and convergence to the final pulse shape for larger detunings was slow, requiring many thousands of passes.

A general conclusion from these results is that instructive results can be obtained for both zero and finite detuning. If however one wishes to obtain more extensive results using this type of direct computer simulation, especially for larger detuning, one needs to use a large number of sample points and some form of convergence algorithm that will lead to faster convergence to steady state than the simple direct modeling used in this work. These results are useful, nonetheless, in indicating the general character of the detuning behavior for larger detuning. We may hypothesize, for example, that the experimentally observed decrease in power output for larger detuning results, at least partly, from spectral broadening causing a decrease in effective gain.

IV. Simplified Analysis for Zero Detuning

The foreword to Hamming's well-known book on numerical analysis [15] gives the maxim:

"The purpose of computing is insight, not numbers."

The work reported in this paper might serve as a case study of this principle. The numerical computations described in the previous section were initially undertaken primarily to provide "numbers." The numerical results, however, also provided insight which led to the simplified analysis presented in this section. In this section, we show how one can simplify the

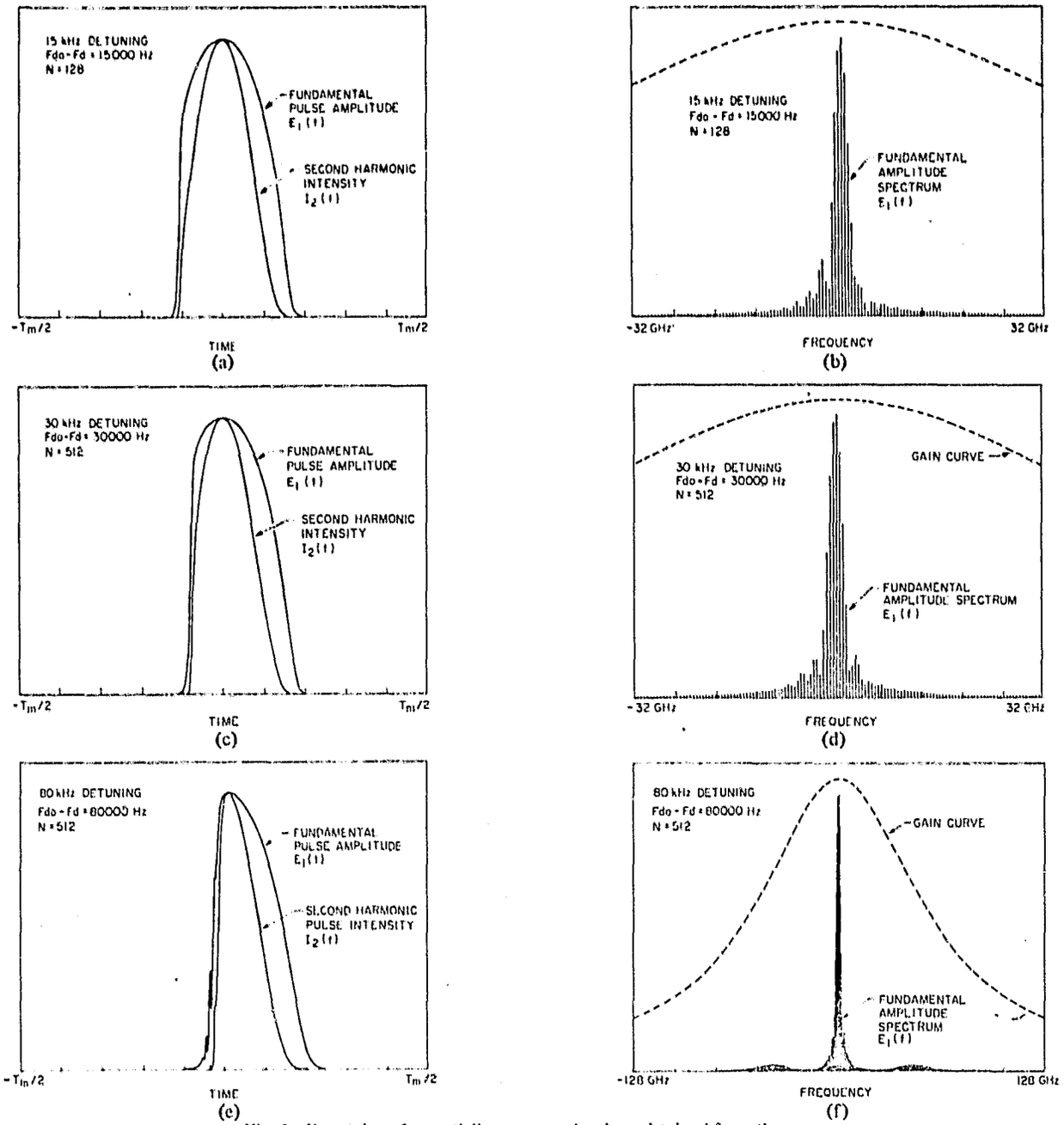

Fig. 3. Examples of essentially converged pulses obtained from the computer simulation process for three increasing amounts of modulation-frequency detuning with otherwise the same parameters as Fig. 2. Note that for the laser in question a detuning of 15 kHz would be equivalent to a cavity length change of $\sim 10\ \mu$m.

physical model so as to obtain much simpler analytic expressions for the performance characteristics of the mode-locked and frequency-doubled laser.

A. Simplified Analysis

The computer results of the previous section make clear that, for zero detuning, the mode-locked pulse spectrum $E_1(f)$ is very narrow compared to the atomic linewidth, while the pulse shape $E_1(t)$ is wide but essentially truncates outside a certain range. We conclude from this that the very wide atomic linewidth of the Nd:YAG laser medium is essentially irrelevant. For the pulse shapes occurring in the frequency-doubled laser, the atomic medium may be modeled as simply an infinite-bandwidth amplifying medium with gain equal to its saturated midband value.

The pulse roundtrip transformation can then be described entirely in the time domain. On a differential basis, the net change in fundamental pulse amplitude $E_1(t)$ in one roundtrip may be written as

$$\Delta E_1(t) = [2g - 2\alpha - 2\delta \sin^2(\pi f_m t) - a_2 I_1(t)]\, E_1(t)$$
$$= 0 \quad \text{for steady-state operation.} \tag{26}$$

Hence, the fundamental pulse shape must be given by

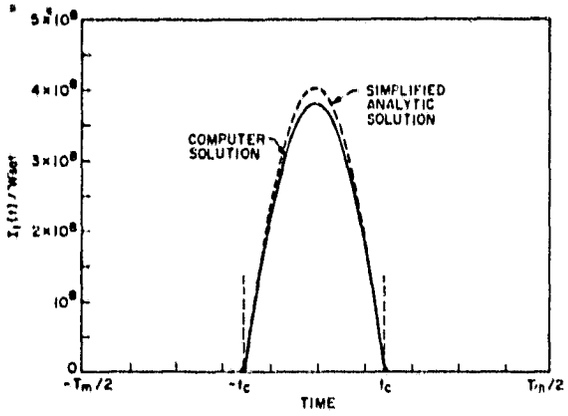

Fig. 4. Zero-detuning pulse shape given by the analytical approximation of (27), compared to the computer simulation results for the same case, with no adjustable parameters. The two pulse shapes are essentially identical.

$$I_1(t) = \frac{2g - 2\alpha - 2\delta \sin^2(\pi f_m t)}{a_2}, \quad |t| \leq t_c \tag{27}$$

and $I_1(t) = 0$ for $|t| > t_c$, where the cutoff points $t = \pm t_c$ at which the pulse amplitude goes to 0 are given by

$$t_c = \frac{T_m}{\pi} \sin^{-1}\left(\frac{g - \alpha}{\delta}\right)^{1/2}, \quad t_c \leq T_m/2. \tag{28}$$

The pulse shape is that shape which must make the net round-trip gain equal to 0 at each instant of time, including the nonlinear effect of the SHG conversion process.

These concepts of essentially infinite bandwidth and zero net gain have been stated previously, especially by Bernecker [4]. However, the consequences do not seem to have been systematically followed up as is done here. As a test of the validity of (27), Fig. 4 shows a comparison of the analytical results of (27) with the "exact" result of the computer simulation from Fig. 2, with no adjustable parameters in either case. The analytic approximation (27) is evidently an excellent approximation to the real pulse. The cutoff points at which the net gain equals 0 are also indicated in the figure.

Equation (27) for the pulse intensity can be integrated over the pulsewidth ($-t_c \leq t \leq t_c$) to obtain the fundamental-frequency pulse energy

$$W_1 = [(4g - 4\alpha - 2\delta) + 2\delta \operatorname{sinc}(2\pi f_m t_c)]\, t_c/a_2 \tag{29}$$

and also the second-harmonic pulse energy

$$W_2 = [(4g - 4\alpha - 2\delta)^2 + 4\delta(4g - 4\alpha - 2\delta) \operatorname{sinc}(2\pi f_m t_c) + 2\delta^2(1 + \operatorname{sinc}(4\pi f_m t_c))]\, t_c/a_2 \tag{30}$$

where $\operatorname{sinc} x \equiv (\sin x)/x$.

The pulse parameters given by (27)–(30) depend on the saturated gain coefficient g. The saturated gain coefficient however depends on the fundamental pulse energy through the saturation relationship (5). A self-consistent set of solutions for the pulse energies W_1 and W_2, the saturated gain g, and all the other pulse parameters can be found in terms of the basic laser parameters a_2, α, δ, f_m, g_0, and W_{sat} by simply iterating (28), (29), and (5) starting with an arbitrary trial value of g.

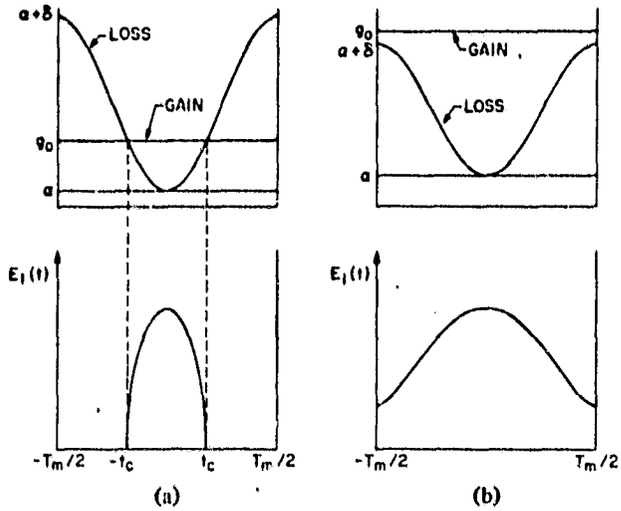

Fig. 5. (a) If the maximum possible gain g_0 in the laser medium is less than the maximum loss $\alpha + \delta$, which occurs at the modulation period edges, then the laser pulse will be cut off at a finite point $t = t_c < T_m/2$ under all operating conditions. (b) If the maximum gain g_0 is greater than $\alpha + \delta$, then under certain operating conditions with large nonlinearity the pulse cutoff points move out to $t_c = T_m/2$, and the laser intensity does not actually drop to 0 between pulses.

This procedure is easily carried out on a small programmable hand calculator or desk calculator.

The above analysis does require extension in one minor respect, as illustrated in Fig. 5(a) and (b). In the limit of large enough nonlinearity a_2, the circulating power in the laser cavity will always become small, and the saturated gain will approach the unsaturated value g_0. So long as the unsaturated gain g_0 is less than the maximum loss $\alpha + \delta$, which occurs at the outer edges of the modulation cycle, i.e., at $t = \pm T_m/2$, then the zero-gain point or pulse cutoff point t_c will always occur somewhere within the modulation period, i.e., for $t_c < T_m/2$, so that the pulse will have a definite cutoff point. If $g_0 > \alpha + \delta$, however, so that the unsaturated gain g_0 can exceed the loss even at the edges of the modulation period, then the pulse cutoff points $\pm t_c$ can move out until they bump into each other at the outer edges of the modulation cycle, i.e., at $\pm T_m/2$. Beyond this point, the laser intensity no longer drops to zero between "pulses," and (28) for t_c is no longer meaningful. We will refer to this as the "no cutoff" condition. In this case, (27)–(30) still remain valid except that t_c must be clamped at the value $T_m/2$. The iterative routine that solves for g, t_c, W_1, and W_2 is easily modified to handle this minor complication.

B. Typical Analytical Results

Figs. 6 and 7 show the fundamental circulating power W_1/W_{sat}, the cutoff t_c, the SHG conversion efficiency $\alpha_{SHG} = W_2/W_1$, and the harmonic extraction efficiency η_2, all as given by the simplified analysis versus the nonlinearity parameter $a_2 W_{sat}$ shown for two typical cases. The second case illustrates the "no cutoff" behavior that occurs for $g_0 > \alpha + \delta$ at large a_2. Note that these results predict the laser's pulse performance entirely in terms of basic laser parameters, namely g_0, α, δ, f_m, and $a_2 W_{sat}$. In particular, the second-harmonic con-

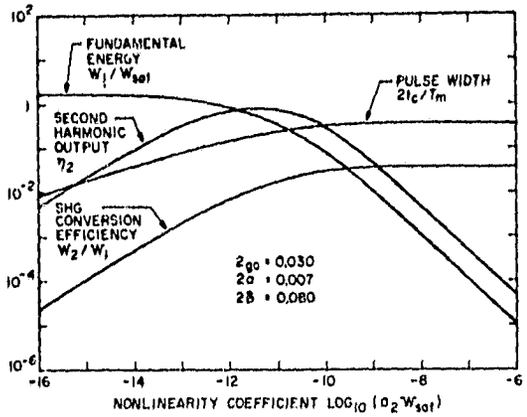

Fig. 6. Variation of laser pulse parameters with nonlinearity coefficient $a_2 W_{sat}$ for a typical laser with parameters as shown (single-pass power gain = 3 percent, single pass cavity loss = 0.7 percent, single-pass modulator index = 8 percent peak-to-peak). This laser always operates in the fully cutoff condition since $g_0 < \alpha + \delta$.

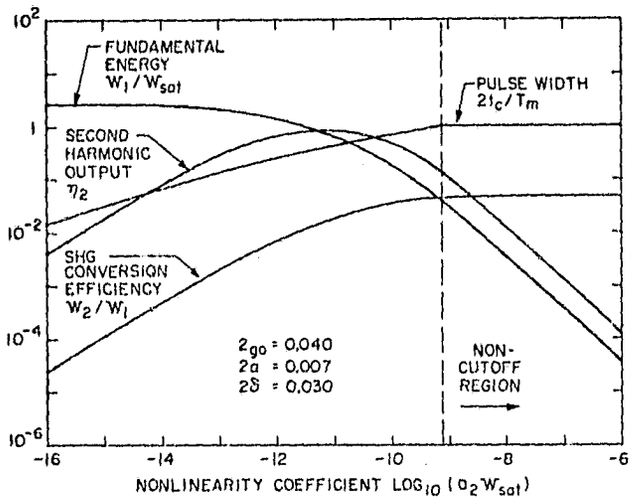

Fig. 7. Variation of laser pulse parameters versus nonlinearity coefficient $a_2 W_{sat}$ for a laser with $g_0 > \alpha + \delta$, showing the "no cutoff" regime of operation at large enough a_2.

version efficiency $\alpha_{SHG} \equiv W_2/W_1$ appears here as a dependent variable rather than an independent variable as in earlier analyses [5], [7]. The results given here are essentially analytic in that iteration of the analytic formulas (28)–(30) can be handled at the programmable calculator level.

For a pulse having the shape of (27) with a base width anywhere in the fully cutoff region $t_c \leq T_m/2$, the fundamental pulsewidth (FWHM) is given by

$$\tau_{p1} = \frac{2T_m}{\pi} \sin^{-1}\left[2^{-1/2} \sin(\pi t_c/T_m)\right]. \tag{31}$$

The harmonic pulsewidth (FWHM) is given by

$$\tau_{p2} = \frac{2T_m}{\pi} \sin^{-1}\left[\left(\frac{2^{1/2}-1}{2^{1/2}}\right)^{1/2} \sin(\pi t_c/T_m)\right]. \tag{32}$$

Hence, we will plot only t_c in the remainder of this paper.

C. Further Analytic Approximations

Further approximations and simplifications of the zero-detuning formulas in (27)–(30) are easily made in various limiting cases, so as to produce various useful and entirely analytic results. For brevity, the details of these results have been deferred to the Appendix.

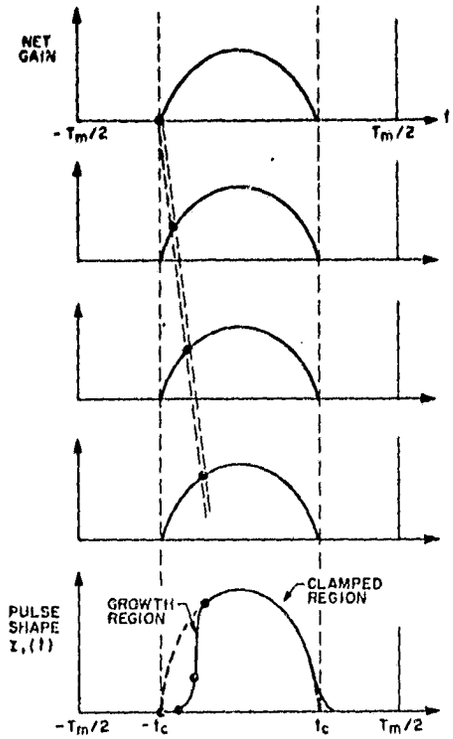

Fig. 8. Sketch illustrating how the circulating pulse intensity at any relative time t during the modulation period with a finite detuning can be traced back to a noise burst originating at the relative time $t = -t_c$ several roundtrips earlier. The super-exponential growth of this noise burst leads to the sharp edge on the pulse, as in the bottom curve. Harmonic generation then clamps the remainder of the pulse at its usual undetuned value.

V. Simplified Detuning Analysis

The simplified analysis of the previous section can be extended to take into account detuning effects. The analytical approach in this case is based on the physical model outlined in Fig. 8. The solid curve on each line of this figure (except the bottom one) shows the net gain, i.e., the laser gain minus the fixed plus time-varying losses, as a function of relative time t within the modulation cycle. "Relative time" here means time measured within each modulation period with respect to the center of that period, so that t is limited to the range $|t| \leq T_m/2$. Suppose the laser has been detuned so that the laser cavity is slightly longer than the on-resonance value. Then a small segment or "packet" of laser energy that passes through the intracavity modulator at a certain relative time t during one modulation cycle will return to the modulator at a slightly later relative time $t + t_d$ during the next modulation cycle, and will pass through the modulator at progressively later times on subsequent cycles. The added time delay t_d per pass is related to the frequency detuning f_d by

$$t_d = \frac{f_{d0} - f_d}{f_m^2}. \tag{33}$$

The dashed lines in Fig. 8 show, for example, how a small

packet of noise energy originating at the zero-gain point $t = -t_c$ will move outward into higher gain regions on successive roundtrips. This packet of energy will be amplified more strongly on each successive pass, until it grows to an intensity sufficient to produce significant harmonic conversion, which will tend to limit its further growth.

Now, in steady-state operation, the output laser pulse $I_1(t)$ is a stationary function—that is, the intensity at any given relative time t during a cycle is constant from cycle to cycle. Fig. 8 shows that the intensity $I_1(t)$ at any relative time t during the modulation cycle can be traced back to the noise energy that originated at relative time $t \approx -t_c$, a number $(t + t_c)/t_d$ of roundtrips earlier. To phrase this in another way, the evolution of the initial noise packet in Fig. 8 as it walks its way across the modulation cycle on successive passes *is just the intensity profile* $I_1(t)$ *of the detuned laser pulse*. The characteristic sharp leading edge seen in the detuned computer results of Fig. 3 represents the rapid "super-exponential" growth from noise of the initial noise packet. This packet grows exponentially, with increasing exponent, until it reaches the level where harmonic generation stabilizes its amplitude. Similarly, the delayed trailing edge in the finite-detuning case represents the packet walking past the zero-gain point $t = +t_c$ on the trailing edge of the modulation cycle and rapidly dying away.

Based on this explanation, we note that the intensity gain of a packet in one roundtrip around the cavity for a packet hitting the mode-locking modulator at relative time t during the modulation cycle will be

$$\Delta I_1 = [4g - 4\alpha - 4\delta \sin^2 (\pi f_m t) - 2a_2 I_1(t)]\, I_1(t). \tag{34}$$

But in the stationary pulse intensity picture the change in intensity ΔI_1 is also the change in $I_1(t)$ between relative time t and relative time $t + t_d$. Hence, we can write this as a differential equation in *relative* time t in the form

$$\frac{1}{I_1}\frac{\Delta I_1}{t_d} \approx \frac{1}{I_1}\frac{dI_1}{dt} = \frac{4g - 4\alpha - 4\delta \sin^2 (\pi f_m t) - 2a_2 I_1(t)}{t_d} \tag{35}$$

since t_d is by definition the change in relative arrival time for one roundtrip. This equation can be integrated in part to give

$$I_1(t) = I_1(-t_c) \exp\left\{t_d^{-1}\left[(4g - 4\alpha - 2\delta)(t + t_c) + (\delta/\pi f_m)(\sin(2\pi f_m t) + \sin(2\pi f_m t_c)) - 2a_2 \int_{-t_c}^{t} I_1(t)\, dt\right]\right\}. \tag{36}$$

This equation can then be integrated numerically to find $I_1(t)$ given an initial noise value for $I_1(t)$ at $t = -t_c$. The exact initial noise value is not at all critical. Fig. 9 shows a detuned laser pulse calculated by integrating (36) for a frequency offset $f_d = 0$ Hz and $2g = 0.0233$. The close comparison with the computer result of Fig. 3 is evident.

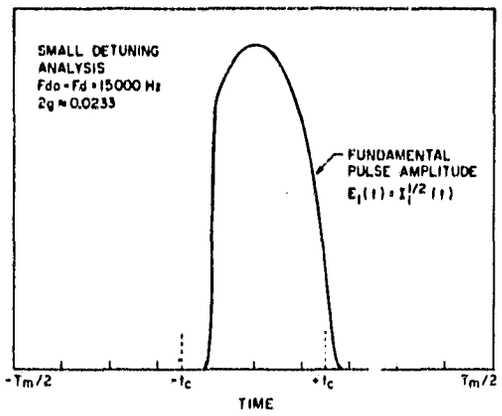

Fig. 9. Example of a detuned fundamental frequency laser pulse calculated using (36), to be compared with computer result in Fig. 3.

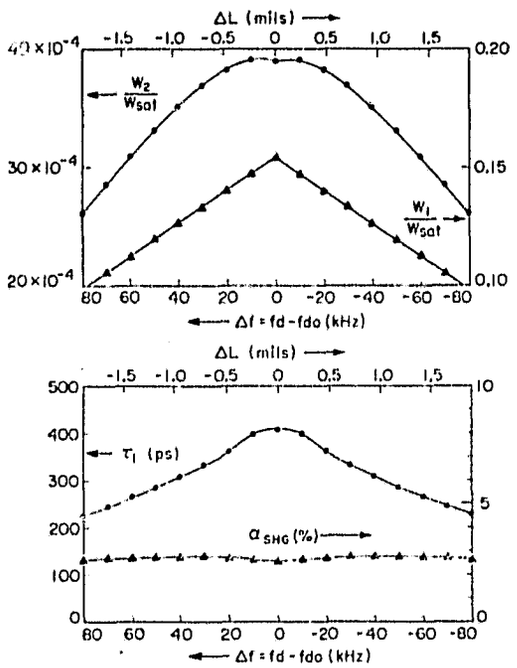

Fig. 10. Typical variation of laser parameters versus detuning as predicted by the simplified analysis of Section V of the text, for the same laser parameters as in other examples in this paper.

The detuned laser performance can then be found, in general, by the following iterative procedure. Starting with a specified set of laser parameters, an initial estimate for the saturated gain g, and an initial noise estimate for $I_1(-t_c)$, (36) is integrated to find $I_1(t)$ and hence the pulse energy W_1. A new value of saturated gain g is then found from (5), and used again in (36). This process is repeated until it converges to give final values of W_1, W_2, and other pulse parameters. The procedure can then be repeated for a new detuning or new values of other basic laser parameters.

Fig. 10 illustrates the behavior of the major pulse parameters versus detuning for a typical case as predicted by this analysis. In calculating the results shown in Fig. 10, we used an initial noise intensity $I_1(-t_c)$ equal to 10^{-10} times the peak intensity, after verifying that the results did not change significantly for variations as large as 3-5 orders of magnitude in the starting noise level.

The general detuning behavior shown in Fig. 10 appears to be in close qualitative and even quantitative agreement with unpublished experimental results [9]. That is, the fundamental pulsewidth τ_{pl} decreases steadily with increasing detuning because of the sharp edge produced on either the leading or trailing edge of the pulse due to the processes described in Fig. 8. The fundamental pulse energy also falls off monotonically, presumably because of the same pulse clipping. At the same time, the conversion efficiency actually increases slightly, probably because the changed pulse shape means the fundamental pulse spends more of its total time at high intensities. The peak pulse intensity may also rise slightly. As a result, the second-harmonic pulse energy falls off somewhat more slowly. Our analysis even gives some indication of a slight increase in second-harmonic energy output for very small detunings. Similar effects have also been seen experimentally [9]. However, some caution must be exercised because of the difficulty in controlling tightly all of the possibly significant effects (e.g., nonlinear absorption in the SHG crystal) that can occur in real lasers.

VI. Conclusion

We believe the analysis and the physical processes described in this paper give a good description of the primary effects controlling both the zero-detuning performance and the detuning behavior of the mode-locked and intracavity frequency-doubled laser under conditions typical of the CW Nd:YAG laser. The analyses are simple enough that results should be readily obtainable for other sets of laser parameters. In accordance with experimental experience, the nonlinearity of the SHG is not particularly critical, while the detuning behavior is extremely critical.

Appendix
Analytic Results for Zero Detuning

This appendix presents several useful analytic approximations derived from the zero-detuning formulas of (27)–(30) in various limiting cases.

A. Large Nonlinearity

For the limiting case of very large nonlinearity, $a_2 \to \infty$, the circulating fundamental pulse intensity W_1 becomes very small, and hence the gain approaches its unsaturated value $g \approx g_0$. The pulsewidth then approaches either the cutoff value

$$t_c \approx \frac{1}{\pi f_m} \sin^{-1}\left(\frac{g_0 - \alpha}{\delta}\right)^{1/2} \tag{A1}$$

in the finite cutoff case $g_0 < \alpha + \delta$, or else the value $t_c = T_m/2$ in the noncutoff case $g_0 > \alpha + \delta$; In either case, the pulse energies approach the limiting values

$$\begin{aligned} W_1 &= [(4g_0 - 4\alpha - 2\delta) + 2\delta \operatorname{sinc}(2\pi f_m t_c)]\ t_c/a_2 \\ W_2 &= [(4g_0 - 4\alpha - 2\delta)^2 + 4\delta(4g_0 - 4\alpha - 2\delta)\operatorname{sinc}(2\pi f_m t_c) \\ &\quad + 2\delta^2(1 + \operatorname{sinc}(4\pi f_m t_c))]\ t_c/a_2 . \end{aligned} \tag{A2}$$

The primary conclusion here is that W_1 and W_2 vary as a_2^{-1} for large a_2, while t_c and α_{SHG} approach constant values, as shown in Figs. 6 and 7.

B. Noncutoff Behavior

For lasers with unsaturated gain $g_0 > \alpha + \delta$, the pulse cutoff point t_c bumps into the edge of the modulation period, $t_c = T_m/2$, above a certain value of the nonlinearity, call it $a_2 = a_{2m}$, so that the laser intensity $I_1(t)$ no longer drops to zero between "pulses". The fundamental and harmonic pulse energies for $a_2 > a_{2m}$ are given by

$$\begin{aligned} W_1 &= (4g - 4\alpha - 2\delta)\, T_m/2a_2 \\ W_2 &= [(4g - 4\alpha - 2\delta)^2 + 2\delta^2]\ T_m/2a_2 . \end{aligned} \tag{A3}$$

However, the saturation formula for the gain g may be written as

$$\frac{W_1}{W_{sat}} = \frac{g_0 - g}{2g} . \tag{A4}$$

Eliminating W_1 between (A3) and (A4) gives the noncutoff relationship

$$a_2 = \frac{(4g - 4\alpha - 2\delta)\, gT_m}{(g_0 - g)\, W_{sat}} . \tag{A5}$$

The noncutoff range of g is $\alpha + \delta < g < g_0$ or $a_2 \geq a_{2m}$, with the lower end of this range being given by $g = \alpha + \delta$ and hence by

$$a_{2m} = \frac{2\delta(\alpha + \delta)\, T_m}{(g_0 - \alpha - \delta)\, W_{sat}} . \tag{A6}$$

This value is the boundary between cutoff and noncutoff regions marked by the dashed vertical line in Fig. 7.

If the modulation index δ is reduced to 0, the laser is always in the noncutoff regime for all values of a_2, i.e., it runs CW rather than mode locked. The analytical results above are still valid, however, and in fact they connect smoothly with the analysis developed by Smith [16] for the CW nonmode-locked laser with intracavity frequency doubling.

C. Quadratic Pulse Approximation

The most important limiting case in practice is the case in which the modulation depth δ is sufficiently large compared to the excess gain $g - \alpha$ to produce a comparatively narrow pulse with $t_c \lesssim T_m/4$. In this limit we may make the approximation $\sin(\pi f_m t) \approx \pi f_m t$ for $|t| \leq t_c$, so that the pulse shape becomes the quadratic approximation

$$I_1(t) \approx \frac{2(g - \alpha) - 2\delta(\pi f_m)^2 t^2}{a_2} , \qquad |t| \leq t_c . \tag{A7}$$

The various pulse parameters are then given by

$$\begin{aligned} t_c &\approx \frac{(g - \alpha)^{1/2}}{\pi f_m \delta^{1/2}} \\ W_1 &\approx \frac{8}{3\pi a_2} \frac{(g - \alpha)^{3/2}}{f_m \delta^{1/2}} \\ W_2 &\approx \frac{128}{15\pi a_2} \frac{(g - \alpha)^{5/2}}{f_m \delta^{1/2}} . \end{aligned} \tag{A8}$$

A common factor in all of these expressions is $(g - \alpha)$. However, this factor is related to the harmonic conversion ratio α_{SHG} by

$$\alpha_{SHG} \approx (16/5)(g - \alpha). \tag{A9}$$

Hence, all of the above quantities can be directly related to α_{SHG} as was done in several earlier analyses [5]-[7].

More basic results can be obtained by using the gain saturation formula (5) or (A4). One can then pick matching values of W_1 and g from (A4); obtain the corresponding value of a_2 from the middle one of (A8); and obtain all the remaining pulse parameters from the remainder of (A7)-(A9).

D. Small Nonlinearity

For small nonlinearity $a_2 \to 0$, the laser will always be in the quadratic pulse limit, assuming a finite modulation depth $\delta > 0$ and hence a finite a_{2m}. From (A7) and (A8), the limit as $a_2 \to 0$ requires $(g - \alpha) \to 0$ to keep W_1 finite. Making $g \approx \alpha$ requires, from (A4)

$$\frac{W_1}{W_{sat}} \approx \frac{g_0 - \alpha}{2\alpha}. \tag{A10}$$

Using this in the middle equation of (A8) then gives

$$(g - \alpha)^{3/2} \approx \left[\frac{3\pi\delta^{1/2}(g_0 - \alpha)W_{sat}}{16\alpha T_m}\right] a_2 \approx K a_2 \tag{A11}$$

where K depends on the laser parameters as shown. The other pulse parameters are then given by

$$t_c \approx \frac{K^{1/3} T_m}{\pi\delta^{1/2}} a_2^{1/3}$$

$$W_2 \approx \frac{128 K^{5/3} T_m}{15\pi\delta^{1/2}} a_2^{2/3}$$

$$\alpha_{SHG} \approx \frac{16 K^{2/3}}{5} a_2^{2/3}. \tag{A12}$$

Figs. 6 and 7 confirm the $a_2^{1/3}$ and $a_2^{2/3}$ variation of these quantities at low a_2.

E. Optimum Pulse Results

For most applications, optimum laser performance is probably considered to be maximum second-harmonic output W_2, even though this does not quite correspond to the shortest pulsewidth τ_{p1} or τ_{p2}. Within the quadratic pulse approximation, (A8) and (A4) can be manipulated to give

$$\frac{W_2}{W_{sat}} = \frac{8(g - \alpha)(g_0 - g)}{5g}. \tag{A13}$$

Optimum harmonic power output thus occurs at the saturated gain value

$$g(\text{opt}) \approx (g_0\alpha)^{1/2}. \tag{A14}$$

The other pulse parameters for this optimum SHG output are then given, in terms of basic laser parameters only, by

$$a_2(\text{opt}) \approx \frac{16\alpha[(g_0\alpha)^{1/2} - \alpha]^{1/2}}{3\pi f_m \delta^{1/2} W_{sat}}$$

$$\frac{t_c(\text{opt})}{T_m} \approx \frac{[(g_0\alpha)^{1/2} - \alpha]^{1/2}}{\pi\delta^{1/2}}$$

$$\frac{W_1(\text{opt})}{W_{sat}} \approx \frac{(g_0\alpha)^{1/2} - \alpha}{2\alpha}$$

$$\frac{W_2(\text{opt})}{W_{sat}} \approx \frac{8[(g_0\alpha)^{1/2} - \alpha]^2}{5\alpha}$$

$$\alpha_{SHG}(\text{opt}) \approx \frac{16}{5}[(g_0\alpha)^{1/2} - \alpha]. \tag{A15}$$

The maximum efficiency with which the frequency-doubled laser can convert the available energy from the laser medium into harmonic output at the optimum operating point is thus

$$\eta_2(\text{opt}) = \frac{W_2(\text{opt})}{2g_0[1 - (\alpha/g_0)^{1/2}]^2 W_{sat}} = 0.8. \tag{A16}$$

The factor of 0.8 represents exactly the inherent efficiency factor for pulsed frequency doubling as defined by Bernecker [4] and Kennedy [8].

Note that none of these optimized results depend (to this degree of approximation) on the modulation frequency f_m; and only the normalized pulsewidth t_c/T_m depends on the modulation index δ. Examination of (A15) shows that the normalized pulsewidth is given to a good first approximation by $t_c/T_m \approx (\frac{1}{2}\pi)(g_0/\delta)^{1/2}$ with a very slow dependence on α/g_0 over the range $0.05 < \alpha/g_0 < 0.6$.

ACKNOWLEDGMENT

One of us (AES) appreciates extensive discussions with D. Radecki and A. Kramer of the Electro-Optics Organization, GTE Sylvania, Mountain View, CA, where this problem initially arose as a consulting assignment.

REFERENCES

[1] T. R. Gurski, "Simultaneous mode-locking and second-harmonic generation by the same nonlinear crystal," *Appl. Phys. Lett.*, vol. 15, pp. 5-6, July 1969.

[2] C. B. Hitz and L. M. Osterink, "Simultaneous intracavity frequency doubling and mode-locking in a Nd:YAG laser," *Appl. Phys. Lett.*, vol. 18, pp. 378-380, May 1971.

[3] R. R. Rice and G. H. Burkhardt, "Efficient mode-locked frequency-doubled operation of an Nd:$YALO_3$ laser," *Appl. Phys. Lett.*, vol. 19, pp. 225-227, Oct. 1971.

[4] O. Bernecker, "Limitations for mode-locking enhancement of internal SHG in a laser," *IEEE J. Quantum Electron.*, vol. QE-9, pp. 897-900, Sept. 1973.

[5] J. Falk, "A theory of the mode-locked, internally frequency-doubled laser," *IEEE J. Quantum Electron.*, vol. QE-11, pp. 22-31, Jan. 1975.

[6] C. J. Kennedy, "A comment on the theory of mode-locking and frequency doubling," *IEEE J. Quantum Electron.*, vol. QE-11, pp. 793-794, Sept. 1975.

[7] C. J. Kennedy, "Frequency-domain analysis of the mode-locked and frequency-doubled homogeneous laser," *IEEE J. Quantum Electron.*, vol. QE-11, pp. 857-862, Nov. 1975.

[8] C. J. Kennedy, "Mode-locked and frequency-doubled laser efficiencies," *Appl. Opt.*, vol. 15, pp. 2955-2956, Dec. 1976.

[9] D. Radecki and A. Kramer, GTE Sylvania, Electro-Optics Organization, Mountain View, CA, private communication.

[10] *Digital Signal Processing*, L. R. Rabiner and C. M. Rader, Eds. New York: IEEE Press, 1972.

[11] E. Oran Brigham, *The Fast Fourier Transform*. Englewood Cliffs, New Jersey: Prentice-Hall, 1974.

[12] R. H. Norton and R. Beer, "New apodizing functions for fourier spectroscopy," *J. Opt. Soc. Amer.*, vol. 66, pp. 259-264, Mar. 1976.

[13] A. E. Siegman and D. J. Kuizenga, "Active mode-coupling phe-

nomena in pulsed and continuous lasers," *Opt. Electron.*, vol. 6, pp. 43–66, Jan. 1974.
[14] C. J. Kennedy, "Pulse chirping in a Nd:YAG laser," *IEEE J. Quantum Electron.*, vol. QE-10, pp. 528–530, June 1974.
[15] R. W. Hamming, *Numerical Methods for Scientists and Engineers.* New York: McGraw-Hill, 1962.
[16] R. G. Smith, "Theory of intracavity optical second-harmonic generation," *IEEE J. Quantum Electron.*, vol. QE-6, pp. 215–223, Apr. 1970.
[17] A. E. Siegman, *Introduction to Lasers and Masers.* New York: McGraw-Hill 1971, p. 461.

A. E. Siegman (S'54–M'57–F'66) was born in Detroit, MI, on November 23, 1931. He received the A.B. degree from Harvard College, Cambridge, MA, in 1953, the M.S. degree from the University of California at Los Angeles under the Hughes Cooperative Plan in 1954, and the Ph.D. degree in electrical engineering from Stanford University, Stanford, CA, in 1957.

Since 1956 he has been on the faculty of Stanford University where he directs a research program in lasers and their applications, with particular interest in laser mode locking, picosecond spectroscopy, and laser resonators. He is the inventor of the unstable optical resonator concept widely used in high-power lasers.

Prof. Siegman is a Fellow of the Optical Society of America, and a member of Phi Beta Kappa, Sigma Xi, and the National Academy of Science Engineering. In 1972, together with D. J. Kuizenga, he received the W. R. G. Baker Award of the IEEE TRANSACTIONS during 1971, and in 1977 he received the J. J. Ebers Award of the Institute of Electrical and Electronics Engineers.

Jean-Marc Heritier was born in Sidi-Kacem, Morocco, on February 2, 1956. He received the Diplame d'Ingenieur in 1977 from the Ecole Centrale des Arts et Manufactures de Paris, France, the M.S. degree in applied physics, in 1978, from Stanford University, Stanford, CA. He is currently completing the requirements for the Ph.D. degree in applied physics at Stanford University, studying the picosecond transient grating technique.